Royal Netherlands Institute for Sea Research

This is a postprint of:

Bijleveld, A.I., MacCurdy, R.B., Chan, Y.-C., Penning, E., Gabrielson, R.M., Cluderay, J., Spaulding, E.L., Dekinga, A., Holthuijsen, S., Ten Horn, J., Brugge, M., Gils, J.A. van, Winkler, D.W. & Piersma, T. (2016). Understanding spatial distributions: negative density-dependence in prey causes predators to trade-off prey quantity with quality. *Proceedings of the Royal Society of London. Series B*, 283: 1828

(Supplementary Information at the end of the document)

Published version: dx.doi.org/10.1098/rspb.2015.1557

Link NIOZ Repository: www.vliz.be/en/imis?module=ref&refid=252508

[Article begins on next page]

The NIOZ Repository gives free access to the digital collection of the work of the Royal Netherlands Institute for Sea Research. This archive is managed according to the principles of the Open Access Movement, and the Open Archive Initiative. Each publication should be cited to its original source - please use the reference as presented.
When using parts of, or whole publications in your own work, permission from the author(s) or copyright holder(s) is always needed.

Title: Understanding spatial distributions: Negative density-dependence in prey causes predators to trade-off prey quantity with quality

Running head: Predators trade quantity against quality

Authors: Allert I. Bijleveld[a*], Robert B. MacCurdy[b], Ying-Chi Chan[a], Emma Penning[a], Rich M. Gabrielson[c,d], John Cluderay[e], Eric L. Spaulding[c], Anne Dekinga[a], Sander Holthuijsen[a], Job ten Horn[a], Maarten Brugge[a], Jan A. van Gils[a], David W. Winkler[d], and Theunis Piersma[a,f]

a. NIOZ Royal Netherlands Institute for Sea Research, Department of Coastal Systems, and Utrecht University, P.O. Box 59, 1790 AB Den Burg, The Netherlands
b. Department of Mechanical and Aerospace Engineering, Cornell University, Ithaca, NY 14853, USA
c. Bioacoustics Research Program, Cornell Laboratory of Ornithology, Cornell University, 159 Sapsucker Woods Road, Ithaca, NY 14850, USA
d. Department of Ecology and Evolutionary Biology, Corson Hall, Cornell University, Ithaca, NY 14853, USA
e. NIOZ Royal Netherlands Institute for Sea Research, National Marine Facilities, and Utrecht University, P.O. Box 59, 1790 AB Den Burg, The Netherlands
f. Chair in Global Flyway Ecology, Conservation Ecology Group, Groningen Institute for Evolutionary Life Sciences (GELIFES), University of Groningen, P.O. Box 11103, 9700 CC Groningen, The Netherlands

***Corresponding author**: Allert I. Bijleveld, NIOZ Royal Netherlands Institute for Sea Research, Department of Coastal Systems, PO Box 59, 1790 AB Den Burg, The Netherlands, allert.bijleveld@gmail.com, tel.: +31(0)222 369382 and fax: +31(0)222 319674

Author contributions: AIB, JAvG, and TP designed the study, AIB, YCC, EP, AD, SH, JtH and MB collected the data on prey distributions, and AIB, YCC, EP, RMG, JC, ELS and AD collected the data on predator distributions for which RBM, RMG, JC, ELS, AD and DWW provided the novel tracking method and technical assistance. AIB analysed the data and wrote a first version of the manuscript, and YCC, JAvG, TP and AIB contributed substantially to revisions.

Competing interests: We have no competing interests.

Summary

Negative density-dependence is generally studied within a single trophic level, thereby neglecting its effect on higher trophic levels. The 'functional response' couples a predator's intake rate to prey density. Most widespread is a type II functional response, where intake rate increases asymptotically with prey density; this predicts the highest predator densities at the highest prey densities. In one of the most stringent tests of this generality to date, we measured density and quality of bivalve prey (Edible Cockles *Cerastoderma edule*) across 50 km² of mudflat, and simultaneously, with novel Time-Of-Arrival methodology, tracked their avian predators (Red Knots *Calidris canutus*). Because of negative density-dependence in the individual quality of cockles, the predicted energy intake rates of Red Knots declined at high prey densities (a type IV, rather than a type II functional response). Resource-selection modelling revealed that Red Knots indeed selected areas of intermediate cockle densities where energy intake rates were maximised given their phenotype-specific digestive constraints (as indicated by gizzard mass). Because negative density-dependence is common, we question the current consensus and suggest that predators commonly maximise their energy intake rates at intermediate prey densities. Prey density alone may thus poorly predict intake rates, carrying capacity and spatial distributions of predators.

Key-words: movement ecology, negative density-dependence, optimal foraging, phenotype-limited spatial distribution, predator-prey dynamics, resource-selection modelling, type IV functional response.

Introduction

Negative density-dependence in state has mainly been studied within trophic levels in the context of population regulation [1-4]. As density increases, survival and reproduction decrease to a point that mortality and reproduction are at equilibrium, i.e. demographic carrying capacity [2, 4]. Negative density-dependent survival and reproduction are population processes mediated by individual states (e.g., body mass [3, 5]). As population size increases, intra-specific competition increases and individual body masses decrease, which reduces reproductive output and survival probability [6]. An ignored aspect of these well-studied processes within trophic levels has been the possibility that reduced individual states (body masses) have implications for energy intake rates of foragers at higher trophic levels (Fig. 1).

A key concept linking two trophic levels is the 'functional response', a function that describes how a predator's per capita intake rate varies with prey density [7]. The functional response is fundamental to spatial distribution modelling [2], estimations of carrying capacity [8, 9], and the analysis of population dynamics in predator-prey systems [1]. In the Holling's type II functional response (also known as Holling's disc equation), the most widespread among predators, intake rate increase with prey density towards an asymptote that is set by handling time[10, 11]. Intake rates can also decline at high prey densities, which results in a hump-shaped functional response (a so-called type IV functional response [12]). As reviewed in [10], the decline in intake rate at high prey densities has been attributed to a decrease in predator searching efficiency (e.g., due to increased predator detection, confusion, mobbing), and an increase in associated foraging costs (e.g., due to the accumulation of toxic prey substances, an increased risk of injury, etc.). However, these processes are particular to specific predator-prey systems. Instead, a more general phenomenon is negative density-dependence [13], which can, through a reduction in the energy state of prey, also cause a declining energy intake rate to predators at high prey densities.

84 The consequence of negative density-dependence among prey is that predators are
85 faced with a trade-off between the quantity and quality of their prey [14, 15]. At low prey
86 densities predators have difficulty finding prey, but because of low levels of intra-specific
87 competition these prey have relatively large energy content. At high densities prey are easier
88 to find, but competition is fierce and prey have relatively low energy content. Herbivores are
89 thought to have a type IV functional response because the digestive quality of forage
90 decreases with an increase in biomass and age [16]. Indeed, some species of herbivores have
91 been shown to select foraging locations of intermediate biomass density where they
92 maximized energy intake rates [17, 18]. Conversely, predators (consumers of herbivores and
93 animals of higher trophic levels, Fig. 1) are generally assumed to maximise energy intake
94 rates at the highest prey densities [2, 19].
95 Aiming to provide a stringent test of this generality, we quantified both the spatial
96 distribution in quantity and quality of their bivalve prey (Edible Cockles *Cerastoderma edule*,
97 hereafter called cockles) and foraging distribution of an avian predator (Red Knot *Calidris*
98 *canutus islandica*, hereafter called knots) at high spatial and temporal resolution over a large
99 intertidal area of 50 km^2. We found that with an increase in cockle density, a cockle's relative
100 flesh mass declined (negative density-dependence). We also showed that a type IV functional
101 response best represented these data and predicted that knots would maximise their energy
102 intake rates on intermediate cockle densities. Individual knots have differently sized gizzards,
103 and hence vary in the amount of shell material they are capable of processing [20]. This in
104 turn means that individuals maximize their intake rates at different cockle densities. To test
105 whether knots indeed selected locations of intermediate cockle densities, we tracked the
106 positions of knots with a novel automated tracking methodology [21] providing high spatial
107 resolution (37 m) and temporal resolution (1 Hz) in the position fixes.
108

Material and Methods

STUDY AREA AND BACKGROUND

Our study site was located in the western Dutch Wadden Sea near the uninhabited islet of Griend (53°15'N, 5°15'E) [22]. Griend is surrounded by extensive intertidal mudflats where, during low tide in the non-breeding season, large flocks of knots can be found foraging. In one tidal cycle, knots often fly tens of kilometres in search of buried hard-shelled bivalves or gastropods (*Hydrobia ulvae*) [22, 23]. Due to low densities of alternative prey (Online Supplementary Fig. S1), knots in our study area and period mainly foraged on cockles. This was confirmed by a diet analysis on 32 droppings from different individuals, which we collected in the study area between 10 August and 27 September 2011. In these droppings we found 272 prey items of which 223 were cockles, 46 *H. ulvae*, and the remaining 3 prey items were *Macoma balthica*, *Mytilus edulis* or *Ensis directus*. In terms of flesh mass, cockles contributed to more than 99% of ingested biomass. Consequently, we focus on the interaction between knots and cockles.

Cockles can be found in densities of up to several thousand individuals m^{-2}, and it has been shown that their flesh mass declines with increasing density (negative density-dependence [24, 25]). Knots swallow their prey whole, which limits the size of ingestible cockles to those smaller than 16 mm in length [22]. Additionally, their intake rate is constrained by the rate of processing ingested shell materials [20]. Due to this digestive constraint, knots maximise their energy intake rates by selecting individual cockles with large flesh mass compared to their shell mass [20]. Note that the gizzard mass of knots is flexible and, over the course of a week, reflects the rate of shell mass that it has processed [20].

THE PREDATORS

Between 2 August and 18 September 2011, we tracked 47 knots with the novel and prototype version of the Time-Of-Arrival (TOA) tracking system [21]. We released all birds between 2 and 5 August 2011, after gluing a 7 g tag (<5 % of body mass) to their rump with cyanoacrylate (Online Supplementary Fig. S2A). Nineteen of these birds had been captured on Griend in March 2010 and were released after 1.5 years in captivity, and the other 28 were caught on the nearby islet of Richel (53°17'N, 5°07'E, Online Supplementary Fig. S2B) between 2 and 4 August 2011. Before releasing the birds, we measured the size of their muscular stomach (gizzard) with ultrasound [26] as described in detail by [27]. The average gizzard mass was 7 g (2.0 SD) ranging between 4.0 and 10.4 g.

The tags emitted a radio signal at one second intervals, which could be received by nine stations that were set up at fixed locations in the study area (Online Supplementary Fig. S2B). If at least three of the receiver stations registered the tag signal, the position of the bird was estimated (Online Supplementary Fig. S3) with the arrival times of the signal and locations of the receiver stations [28]. To reduce measurement error, we median-filtered the positioning data with a 7-points sliding window (see R-package "signal"). Because birds moved out of the area, we lost reception of many tags in the course of our study, and because of technical issues, inherent to the use of prototype systems, signal reception at the receiver stations was sometimes intermittent. Therefore, we restrained our statistical analyses to the period between 12 August and 26 August 2011, and excluded data from the receiver stations on Richel. In this period and area we had the most regular tracking data and the most individuals. We collected a total of 1,341,438 estimated positions for 19 different birds (five that were released from captivity and 14 freshly captured).

To identify intensively used areas and to reduce the computational issues associated with this large data set (e.g., time-consuming calculations, serial autocorrelation [29]), we summarised our tracking data in 'residence patches' as follows. We divided an individual's

158 track into sections between two consecutive high tides and calculated residence times for
159 successive positions within these tidal periods [30]. For calculating residence times, we used
160 a time window of 3 h and a patch diameter of 250 m reflecting the grid-spacing for cockle
161 sampling stations. Following [31], we segmented these residence time data automatically and
162 we refer to [30] for details. To exclude the positions of flying birds as well as infrequently
163 used areas, we disregarded segments with a residence time < 10 min (n = 165). For each
164 segment we extracted the median coordinate and residence time. We will refer to each
165 segment as a 'residence patch' indicating both the location and the time spent there.
166 The extent of available mudflat area is restricted by the tide that forces birds to move
167 during parts of the tidal cycle. Because we were interested in foraging behaviour and resource
168 selection without tidal forcing, we restricted our residence-patch data to 3.5 h before and 2.5
169 h after low tide (Online Supplementary Fig. S4). Additionally, we restricted our analyses to
170 individuals with 5 or more calculated residence patches. In total, this procedure resulted in
171 data from 13 individuals with 365 residence patches ranging in duration from 10 min to 4.7 h
172 (using 558,781 estimated locations).
173
174 THE PREY
175 Between 15 and 19 July 2011, we sampled cockle density, flesh mass and shell mass on a 250
176 m sampling grid, complemented by an additional 20% sampling stations randomly placed on
177 the grid lines (Online Supplementary Fig. S2B). This composite sampling design allowed for
178 accurate spatial interpolations of cockle density, flesh mass and shell mass [32], necessary for
179 predicting these variables at locations where knots were recorded foraging. To reduce
180 laboratory time, we measured flesh and shell mass of individual cockles on roughly 25% of
181 the sampling stations (i.e. on 500 m grid spacing). At each sampling site we collected 0.018
182 m^2 of mudflat to a depth of 30 cm. Judging their length in the field, we stored cockles < 8

183 mm in a 4% formaldehyde solution, and froze larger cockles [33]. In the laboratory, we
184 measured their lengths to the nearest 0.1 mm, ash-free dry mass of the flesh ($AFDM_{flesh}$), and
185 dry mass of the shell (DM_{shell}) [22] (for details see Online Supplementary Appendix S1)
186 Overall, we sampled 854 stations and collected 15,874 individual cockles. In total, we
187 obtained 663 estimates for $AFDM_{flesh}$ from 1,721 individuals that we collected from 120
188 sampling cores. For analysing DM_{shell}, we collected data of 82 individuals from 33 sampling
189 stations.

190 $AFDM_{flesh}$, DM_{shell} and their variances increase with cockle length
191 (heteroscedasticity). To compare flesh and shell mass between differently sized cockles, we
192 therefore calculated an individual's relative flesh and shell mass by dividing its measured
193 $AFDM_{flesh}$ or DM_{shell} by the (predicted) length-specific average [24]. These averages were
194 obtained by fitting non-linear local regression models (LOESS with local quadratic fitting)
195 between $AFDM_{flesh}$ or DM_{shell}, and length on logarithmic scales (Online Supplementary Fig.
196 S5). We back-transformed these residuals to reflect an individual's *relative* $AFDM_{flesh}$ and
197 DM_{shell} compared to the average cockle of identical length.

198 For each sampling station, we calculated cockle density by counting the number of
199 cockles and dividing that by the surface area of a sampling core. To normalise model
200 residuals, we transformed these counts with the common logarithm ($\log_{10}$). To avoid taking
201 the logarithm of zero, we added one before the data transformation.

202 We analysed the density dependence on relative $AFDM_{flesh}$ and DM_{shell} in linear
203 mixed-effect models with sampling station as a random effect and cockle density (m^{-2}) as an
204 explanatory variable. We also investigated effects of length and the interaction of length and
205 density on both relative $AFDM_{flesh}$ and DM_{shell}. Cockle length ranged from 1.0 to 41.1 mm.
206 We centred length and $\log_{10}$-transformed density by subtracting their means of 8.9 mm and

207 3.14 respectively. By parametric bootstrapping (n = 1,000), we calculated significance under
208 the null hypothesis that the estimated coefficients are zero.
209
210 INTERPOLATING RESOURCE LANDSCAPES
211 To calculate resource landscapes for foraging knots, we spatially interpolated cockle densities
212 and relative $AFDM_{flesh}$ across the study area. For the interpolation of cockle densities, we
213 selected cockles that knots can swallow (length < 16 mm, [22]). Because many cockles were
214 too small to separate shell from flesh (Online Supplementary Appendix S1), the sample sizes
215 of DM_{shell} were low too low for spatial interpolations. To interpolate cockle density and
216 relative $AFDM_{flesh}$, we calculated correlograms from the measured values and fitted
217 exponential spatial autocorrelation functions (Online Supplementary Fig. S6) [24, 32]. To
218 reduce prediction error in interpolating relative $AFDM_{flesh}$, we included spatially interpolated
219 cockle densities as a covariate.
220 We interpolated measured cockle densities and relative $AFDM_{flesh}$ on spatial grids
221 with a resolution of 25 by 25 m. These resource landscapes were used to predict a knot's
222 energy intake rate by multiplying the functional response (Holling type II) by the interpolated
223 (density-dependent) energy content of cockles: $IR = [(a \times N) / (1 + a \times N \times T_h)] \times e(N)$,
224 where IR is the energy intake rate (mg $AFDM_{flesh}$ s^{-1}), a is searching efficiency (m^2 s^{-1}), N is
225 interpolated cockle density (n m^{-2}), T_h is handling time (s), and e(N) is density-dependent
226 $AFDM_{flesh}$ (mg) of an individual cockle. We used a searching efficiency of 6.4 cm^2 s^{-1} [34],
227 and estimated handling time from video recordings collected between 14 August and 24
228 September. Based on 23 tagged birds handling 637 cockles, handling time was 4.0 s (SD 1.7)
229 which compares well with earlier findings [34]. To calculate e(N), we assumed that knots fed
230 on cockles of 7 mm long, which is the size that knots preferentially selected in this area the
231 previous year [24]. We then multiplied the spatially interpolated measurements of relative

232 $AFDM_{flesh}$ by 1.7 mg (the average $AFDM_{flesh}$ of 7 mm cockles, Online Supplementary Fig.
233 S5A). Note that e(N) [mg] is derived from interpolated measurements of density and relative
234 $AFDM_{flesh}$.

235 We calculated a knot's digestive constraint on shell-mass intake rate (c, mg s^{-1}) as q ×
236 $0.05 \times G^2$ [23], where q is the ratio of $AFDM_{flesh}$ to DM_{shell}, and G is gizzard mass (g).
237 Because the sample size was inadequate for spatially interpolating measurements of DM_{shell},
238 we predicted relative DM_{shell} from interpolated densities with the density-dependent model
239 presented in Online Supplementary Table S1B. To get absolute shell masses, we multiplied
240 relative DM_{shell} by 24.3 mg (the average DM_{shell} for cockles of 7 mm, Online Supplementary
241 Fig. S5B). We then calculated a bird's gizzard-mass-dependent intake rate as the minimum of
242 its predicted intake rate without a digestive constraint (IR) and its digestive constraint c [23].
243 We predicted gizzard-mass-dependent intake rate for average gizzard mass (7 g, $IR_{avg.gizzard}$),
244 and for each individual's measured gizzard mass ($IR_{ind.gizzard}$). Birds with different gizzard
245 masses have different levels of intake rate (Online Supplementary Fig. S7). To compare
246 $IR_{ind.gizzard}$ between birds with different gizzard masses, we standardised $IR_{ind.gizzard}$ by
247 subtracting an individual's mean $IR_{ind.gizzard}$ and dividing it by its standard deviation (Online
248 Supplementary Fig. S8). Large values of $IR_{ind.gizzard}$ reflect areas where individuals would
249 achieve a large intake rate given their gizzard mass.
250
251 RESOURCE SELECTION ANALYSES
252 Within a used-availability design [35], we modelled variation in knot locations as a function
253 of prey-related covariates (cockle density, relative cockle $AFDM_{flesh,}$ predicted intake rates).
254 The values of covariates at the bird's residence patches (used points) are contrasted with
255 those that were available to them (availability points). The null model is that resources are
256 selected proportional to their availability, and that deviations from proportionality indicate

avoidance or preferential selection. We complemented each residence patch with 15 availability locations resulting in a sample size of 5,475 (Online Supplementary Fig. S9). At each used and availability location, we extracted from the resource landscapes: cockle density, relative $AFDM_{flesh}$, and predicted intake rates without a digestive constraint (IR), with an average digestive constraint ($IR_{avg.gizzard}$), and with an individual-specific digestive constraint ($IR_{ind.gizzard}$). We analysed the used (1) and availability (0) data in mixed-effect logistic regression models, thus correcting for variation among individuals. To avoid biased estimates of the resource selection functions, we applied infinitely weighted logistic regression by weighing used locations by 1 and availability locations by 1,000 [36]. We additionally weighted our used locations by their residence time (h). The resource selection function is defined as the exponent of the predictors of the logistic regression model ignoring the intercept, which is proportional to the density of knot locations. For representation purposes, we scaled the resource selection functions between zero and one.

We calculated a null-model (intercept only) for the used-availability data. For each of the five explanatory resource-related covariates, we fitted two additional models with: (1) an intercept and linear predictor, and (2) an intercept, a linear, and a quadratic predictor. The quadratic term can capture possible trade-offs between resources, e.g., between cockle density and relative $AFDM_{flesh}$. High residual spatial and temporal correlation within location observations could lead to overly complex models. We, therefore, used likelihood-based cross validation [37] for selecting between the shapes of resource selection models (i.e. a null-, linear-, or quadratic), see Online Supplementary Table S2.

We analysed our data in R v3.1.0 [38] with the packages ‘ncf’ for calculating correlograms, ‘fields’ for spatial interpolations, ‘lme4’ for mixed-effect model analyses, and ‘adeHabitatLT’ for calculating residence times. We additionally used the packages ‘RODBC’, ‘PBSmapping’, ‘spatstat’, ‘sp’, ‘raster’, ‘signal’, ‘rgdal’, for working with the

(spatial) data. For plotting the spatial data we used QGIS v2.2.0 (http://qgis.osgeo.org). We segmented residence time data with Matlab (code available from http://www.math.u-psud.fr/~lavielle/programmes_lavielle.html).

Results

NEGATIVE DENSITY-DEPENDENCE IN THE PREY

Both the relative flesh mass ($AFDM_{flesh}$) and shell mass (DM_{shell}) of cockles declined with their density (Fig. 2A, and Online Supplementary Table S1). Neither length, nor its interaction with density, significantly affected a cockle's relative $AFDM_{flesh}$ and DM_{shell}. The decline in relative $AFDM_{flesh}$ was stronger than the decline in relative DM_{shell}. For this reason, the ratio of flesh to shell mass (digestive quality) also declined with cockle density. Because of the negative density-dependence among cockles, knots had a type IV functional response (Fig. 2B).

INTERPOLATED RESOURCE LANDSCAPES

Cockle density (Fig. 3A) and relative $AFDM_{flesh}$ (Fig. 3B) were patchily distributed. Consistent with the analysis of negative density dependence (Fig. 2A, and Online Supplementary Table S1A), high cockle densities coincided with low relative $AFDM_{flesh}$ (Fig. 3A, B). With interpolated cockle densities (Fig. 3A) and relative $AFDM_{flesh}$ (Fig. 3B), we predicted intake-rate landscapes for knots without a digestive constraint (IR, Fig. 3C), with an average digestive constraint ($IR_{avg.gizzard}$, Fig. 3D), and with an individual-specific digestive constraint ($IR_{ind.gizzard}$, Online Supplementary Fig. S8). Compared to an unconstrained forager, intake rates of digestively constrained foragers are considerably reduced (Fig. 3D); the smaller the gizzard size the lower its intake rate (Online Supplementary Fig. S7).

RESOURCE SELECTION

The resource selection analyses (Online Supplementary Tables S2 and S3) showed that knots preferentially selected locations of intermediate cockle densities (Fig. 4A). At these locations, the birds encountered cockles with intermediate relative $AFDM_{flesh}$ (Fig. 4B). Likewise, they encountered intermediate predicted intake rates when ignoring the digestive constraint (IR, Fig. 4C) and when considering an average digestive constraint ($IR_{avg.gizzard}$, Fig. 4D). When we incorporated an individual-specific digestive constraint, we found that knots had selected those locations where they maximised their individual gizzard-mass-dependent energy intake rate ($IR_{ind.gizzard}$, Fig. 4E). Birds with large gizzards selected locations with high cockle density but small relative flesh mass, whereas birds with small gizzards selected locations with low cockle density but large relative flesh mass (Online Supplementary Fig. S10).

Discussion

We have shown that negative density-dependence among prey presented their predators with a trade-off between prey quantity and quality. Instead of the general simplification that energy intake rates increase asymptotically with prey density (a type II response), knots feeding on cockles had a type IV functional response. Resource selection analyses confirmed that free-living knots preferentially selected foraging locations with intermediate cockle densities and flesh masses. In fact, knots selected locations where they could maximise their energy intake rates given their phenotype-specific digestive constraint (gizzard mass).

CONSISTENT INDIVIDUAL DIFFERENCES IN HABITAT SELECTION AND PREY QUALITY INGESTION

In the past decade, research on consistent individual differences in behaviour (animal personality) has become popular [39-41]. Animal personality limits behavioural flexibility

and can correlate with individual resource specialisation [42, 43], which can have important ecological, evolutionary, and conservation implications [44]. In knots, personality variation explains variation in gizzard mass, possibly caused by individual specialisation on particular prey qualities [27]. The gizzard mass of knots is flexible and, over the course of a week, reflects the quality of its diet [20]. Birds feeding mainly on high-quality prey maintain small gizzards, while birds mainly feeding on low quality prey maintain large gizzards [26]. That gizzard mass explained resource selection in the current study suggests that knots consistently differ in prey quality ingestion. To guide potential future research improving our understanding of the ecological implications of personality and individual resource specialisation, we will provide three non-mutually exclusive hypotheses to explain why knots differ in habitat selection and ingested prey quality.

(1) At large spatial scales, knots might select foraging locations from habitat characteristics such as prey density, inundation time, and/or predation danger. If knots differ in their preference for certain habitat, and if these habitat characteristics are correlated with prey quality (as they often are, e.g., [14]), knots could consistently ingest particular prey qualities.

(2) At small spatial scales, knots could have developed different diet specialisations during ontogeny [42, 43, 45]. Because high quality prey are more difficult to find than low quality prey, the experience that knots gain feeding on high quality prey could make it easier for these animals to specialise their feeding [27]. Or they could specialise on more readily available low quality prey by adapting their physiology to increase processing efficiency. To specialise on particular prey qualities in the single-prey situation studied here, knots need to sense quality variation between individual cockles. A previous study, in which cockle quality was measured before and after predation by knots, shows that cockles that survived knot

356 predation had relatively little flesh mass and large shell mass [24]. Knots thus appear to be
357 able to somehow sense the quality of an individual cockle.
358 (3) In line with diet specialisation, consistent prey quality ingestion could also
359 originate from competition avoidance [42, 46]. Knots are known to avoid explicit interference
360 competition [47], and, when given a choice between equally accessible and available prey
361 types, they prefer high quality prey [48]. As prey density and quality are inversely related
362 (Fig. 2A), birds compete over the less abundant high-quality prey. As a result, competitively
363 dominant birds would forage in areas with high-quality prey and obtain small gizzards, while
364 competitively subordinate birds would forage in areas with low-quality prey and obtain large
365 gizzards.
366
367 GENERALITY AND CONSEQUENCES OF A TYPE IV FUNCTIONAL RESPONSE
368 Holling's type II functional response is since long thought to be the most widespread among
369 predators [10, 11]. In this study we have shown that negative density-dependence among prey
370 results in a type IV functional response. As negative density-dependence is commonly found
371 among prey [13], we predict that most predators will be faced with type IV functional
372 responses. Until now this might have remained unnoticed because numerical intake rate is
373 often multiplied by an average (size dependent) flesh mass [e.g., 49]. To investigate the effect
374 of negative density-dependence among prey on a predator's intake rate, flesh mass of
375 individual prey should be measured over a range of densities. We will now discuss two main
376 consequences of ignoring negative density-dependence among prey for predicting a
377 predator's energy intake rates. First, predicted energy intake rates are biased. Second,
378 predators are wrongfully assumed to maximise their energy intake rates at the highest prey
379 densities.

Carrying capacity of an area is often defined as the maximum number of predator-days that can be supported by the local standing stock of prey [8, 9]. In the absence of prey growth and recruitment, the number of predators that can be supported depends on their predicted intake rates [9]. Ignoring density-dependence among prey leads to biased predictions of a predator's energy intake rates, which can have consequences for estimating an area's carrying capacity and hence, possibly, management and conservation efforts. In our study, ignoring density dependence would have led to an underestimation of predicted intake rates by as much as 60% on the lowest prey densities and an overestimation by almost 50% on the highest prey densities (Online Supplementary Fig. S11A). Moreover, given the distribution of prey densities in our study, the surface area of suitable knot habitat (where predicted intake rates were above a knot's minimum requirement, Fig. 2B) was overestimated by 12.4% when ignoring negative density-dependence among prey.

Foragers are usually assumed to aggregate where predicted intake rates are highest [2, 19]. The shape of the functional response, therefore, directly determines where predators will aggregate: they are generally assumed to maximise energy intake rates by foraging at the highest prey densities. Including negative density-dependence into the functional response, however, can substantially lower the prey density at which predators are predicted to maximise energy intake rates. How substantial this effect is depends on the strength of negative density-dependence among prey, and on how fast their functional response (without density dependence) levels off with prey density. Searching efficiency, handling time and digestion time are positively related to the rate at which the functional response levels off (Online Supplementary Fig. S11B and C). In the presence of negative density-dependence among prey, predators with high searching efficiencies and long handling or digestion times will maximise energy intake rates at substantially reduced prey densities. Moreover, they will have a pronounced hump in their functional response, i.e. their predicted intake rates at

intermediate prey densities will be substantially larger than those at the highest prey densities (Online Supplementary Fig. S11B and C).

TYPE IV FUNCTIONAL RESPONSE ALLOWS THE 'GARDENING OF PREY'

A type IV functional response may offer interesting predator-prey dynamics. Grazing flocks of Barnacle Geese (*Branta leucopsis),* for instance, have been hypothesized to stimulate renewed protein-rich grass growth, thereby providing opportunity for future foraging on high quality vegetation [50]. Indeed, without lowering biomass, grazing improved the vegetation quality and attracted foraging geese [51]. Consequently, brent geese *Branta bernicla* have been hypothesized to adopt a cyclic grazing pattern that optimizes their protein intake between locations [52]. We can speculate about this 'grazing optimization hypothesis' for predators in the context of our study. Thinning of cockle densities reduces competition among cockles and allows the surviving cockles to accumulate flesh mass. Even though it is highly speculative, knots may optimise energy intake rates by 'gardening' their cockle prey. However, opposite to grazers, predators kill their prey and reduce their density, which thereby become difficult to find [24], which in turn reduces the benefit from such 'gardening'. One way to investigate this 'gardening hypothesis' is to determine whether knots, after thinning cockle densities, allow time for their prey to increase in flesh mass before revisiting these locations [52]. From a (game) theoretical perspective, an interesting question is if, and under what circumstances, gardening prey is an evolutionary stable strategy. For instance, will a gardening strategy be outcompeted by a 'cheater-strategy' where individuals sneak ahead of the flock and harvest the gardened high quality prey? Conversely, cheaters, which separate themselves from the main flock, might incur increased predation costs because they lose the safety of numbers.

Data Accessibility

Data is available in the Dryad Digital Repository [53].

Acknowledgements

This study included the help of very many people. At NIOZ we were helped by Martin Laan, Ruud Groenewegen, Frank van Maarseveen, Mark Eveleens, Marck Smit, Walther Lenting, Hans Malschaert, Bram Fey, Tony van der Vis, Hein de Vries, Wim-Jan Boon, Bernard Spaans, Tanya Compton, Anita Koolhaas, Piet van den Hout, Katja Philippart, Ewout Adriaans, Julia Piechocki, Niamh McSweeney, Jeremy Smith, the many SIBES co-workers, and departmental colleagues. For allowing access to Griend we thank manager Otto Overdijk of the Vereniging Natuurmonumenten. For supplies on Griend, we thank Dirk de Boer and Peter van Tellingen. Also we thank Wouter Splinter, Marleen Feldbrugge, and Jelle Loonstra who were volunteers in the field. We thank Geert Aarts for helping with the resource selection modelling. We additionally thank Thomas Oudman for fruitful discussions and for commenting on an earlier version of the manuscript. We thank John Fryxell and an anonymous referee for their constructive comments on the manuscript. Our work was supported by core funding of NIOZ to TP and grants from NWO-ALW to TP (TOP-grant 'Shorebirds in space', no. 854.11.004), the Waddenfonds to TP (project 'Metawad', WF 209925), and a NWO-VIDI grant to JAvG (no. 864.09.002), as well as funding from ZKO, NWO, NAM, and NIOZ for the benthic sampling programme 'SIBES'. All research was carried out according to Dutch law (DEC licence NIOZ 10.04).

References

1. de Roos A.M., Persson L. 2013 *Population And Community Ecology Of Ontogenetic Development*. Princeton, Princeton University Press; 448 p.

2. Sutherland W.J. 1996 *From individual behaviour to population ecology*. Oxford, Oxford University Press.

3. Turchin P. 1999 Population regulation: a synthetic view. *Oikos* **84**, 153-159. (doi:10.2307/3546876).

4. Sinclair A., Krebs C.J. 2002 Complex numerical responses to top–down and bottom–up processes in vertebrate populations. *Phil Trans R Soc B* **357**, 1221-1231.

5. Sæther B.-E. 1997 Environmental stochasticity and population dynamics of large herbivores: A search for mechanisms. *Trends Ecol Evol* **12**, 143-149.

6. Paine R.T. 1976 Size-limited predation: an observational and experimental approach with the *Mytilus-Pisaster* interaction. *Ecology* **57**, 858-873. (doi:10.2307/1941053).

7. Holling C.S. 1959 Some characteristics of simple types of predation and parasitism. *Can Entomol* **91**, 385-398.

8. Goss-Custard J.D., Stillman R.A., West A.D., Caldow R.W.G., McGrorty S. 2002 Carrying capacity in overwintering migratory birds. *Biol Conserv* **105**, 27-41. (doi:10.1016/S0006-3207(01)00175-6).

9. Sutherland W.J., Anderson C.W. 1993 Predicting the distribution of individuals and the consequences of habitat loss: the role of prey depletion. *J Theor Biol* **160**, 223-230. (doi:10.1006/jtbi.1993.1015).

10. Jeschke J.M., Kopp M., Tollrian R. 2002 Predator functional responses: discriminating between handling and digesting prey. *Ecol Monogr* **72**, 95-112. (doi:10.1890/0012-9615(2002)072[0095:PFRDBH]2.0.CO;2).

11. Skalski G.T., Gilliam J.F. 2001 Functional responses with predator interference: viable alternatives to the Holling type II model. *Ecology* **82**, 3083-3092. (doi:10.1890/0012-9658(2001)082[3083:FRWPIV]2.0.CO;2).

12. Holling C.S. 1961 Principles of insect predation. *Annu Rev Entomol* **6**, 163-182. (doi:10.1146/annurev.en.06.010161.001115).

13. Gurevitch J., Morrow L.L., Wallace A., Walsh J.S. 1992 A meta-analysis of competition in field experiments. *Am Nat* **140**, 539-572.

14. Sutherland W.J. 1982 Spatial variation in the predation of Cockles by Oystercatchers at Traeth Melynog, Anglesey. I. The cockle population. *J Anim Ecol* **51**, 481-489. (doi:10.2307/3978).

15. Sutherland W.J. 1982 Spatial variation in the predation of Cockles by Oystercatchers at Traeth Melynog, Anglesey. II. The pattern of mortality. *J Anim Ecol* **51**, 491-500. (doi:10.2307/3979).

16. Fryxell J.M. 1991 Forage quality and aggregation by large herbivores. *Am Nat*, 478-498.

17. van Beest F.M., Mysterud A., Loe L.E., Milner J.M. 2010 Forage quantity, quality and depletion as scale-dependent mechanisms driving habitat selection of a large browsing herbivore. *J Anim Ecol* **79**, 910-922. (doi:10.1111/j.1365-2656.2010.01701.x).

18. Fryxell J.M., Wilmshurst J.F., Sinclair A.R.E. 2004 Predictive models of movement by serengeti grazers. *Ecology* **85**, 2429-2435. (doi:10.1890/04-0147).

19. Stephens D.W., Brown J.S., Ydenberg R.C. 2007 *Foraging: behavior and ecology*. Chicago, IL, The University of Chicago Press.

20. van Gils J.A., Piersma T., Dekinga A., Dietz M.W. 2003 Cost-benefit analysis of mollusc-eating in a shorebird II. Optimizing gizzard size in the face of seasonal demands. *J Exp Biol* **206**, 3369-3380. (doi:10.1242/jeb.00546).

21. MacCurdy R.B., Gabrielson R.M., Cortopassi K.A. 2011 Automated wildlife radio tracking. In *Handbook of position location: theory, practice, and advances* (eds. Zekavat S.A., Buehrer R.M.), pp. 1129-1167, John Wiley & Sons, Inc.

22. Piersma T., Hoekstra R., Dekinga A., Koolhaas A., Wolf P., Battley P.F., Wiersma P. 1993 Scale and intensity of intertidal habitat use by knots *Calidris canutus* in the Western Wadden Sea in relation to food, friends and foes. *Neth J Sea Res* **31**, 331-357.

23. van Gils J.A., Dekinga A., Spaans B., Vahl W.K., Piersma T. 2005 Digestive bottleneck affects foraging decisions in red knots *Calidris canutus*. II. Patch choice and length of working day. *J Anim Ecol* **74**, 120-130. (doi:10.1111/j.1365-2656.2004.00904.x).

24. Bijleveld A.I., Twietmeyer S., Piechocki J., van Gils J.A., Piersma T. 2015 Natural selection by pulsed predation: survival of the thickest. *Ecology* **96**, 1943-1956. (doi:10.1890/14-1845.1).

25. Jensen K.T. 1993 Density-dependent growth in cockles (*Cerastoderma edule*): evidence from interannual comparisons. *J Mar Biol Assoc UK* **73**, 333-342.

26. Dekinga A., Dietz M.W., Koolhaas A., Piersma T. 2001 Time course and reversibility of changes in the gizzards of red knots alternately eating hard and soft food. *J Exp Biol* **204**, 2167-2173.

27. Bijleveld A.I., Massourakis G., van der Marel A., Dekinga A., Spaans B., van Gils J.A., Piersma T. 2014 Personality drives physiological adjustments and is not related to survival. *Proc R Soc B* **281**, 20133135. (doi:10.1098/rspb.2013.3135).

28. Piersma T., MacCurdy R., Gabrielson R., Cluderay J., Dekinga A., Spaulding E., Oudman T., Onrust J., van Gils J., Winkler D.W., et al. 2014 Fine-scale measurements of individual movements within bird flocks: the principles and three applications of TOA tracking. *Limosa* **87**, 156-167.

29. Aarts G., MacKenzie M., McConnell B., Fedak M., Matthiopoulos J. 2008 Estimating space-use and habitat preference from wildlife telemetry data. *Ecography* **31**, 140-160. (doi:10.1111/j.2007.0906-7590.05236.x).

528 30. Barraquand F., Benhamou S. 2008 Animal movements in heterogeneous landscapes:
529 identifying profitable places and homogeneous movement bouts. *Ecology* **89**, 3336-3348.
530 (doi:10.1890/08-0162.1).
531 31. Lavielle M. 2005 Using penalized contrasts for the change-point problem. *Signal*
532 *Process* **85**, 1501-1510. (doi:10.1016/j.sigpro.2005.01.012).
533 32. Bijleveld A.I., van Gils J.A., van der Meer J., Dekinga A., Kraan C., van der Veer
534 H.W., Piersma T. 2012 Designing a benthic monitoring programme with multiple conflicting
535 objectives. *Methods Ecol Evol* **3**, 526-536. (doi:10.1111/j.2041-210X.2012.00192.x).
536 33. Compton T.J., Holthuijsen S., Koolhaas A., Dekinga A., ten Horn J., Smith J.,
537 Galama Y., Brugge M., van der Wal D., van der Meer J., et al. 2013 Distinctly variable
538 mudscapes: distribution gradients of intertidal macrofauna across the Dutch Wadden Sea. *J*
539 *Sea Res* **82**, 103-116. (doi:10.1016/j.seares.2013.02.002).
540 34. Piersma T., van Gils J., de Goeij P., van der Meer J. 1995 Holling's functional
541 response model as a tool to link the food-finding mechanism of a probing shorebird with its
542 spatial distribution. *J Anim Ecol* **64**, 493-504.
543 35. Manly B.F.J., McDonald L.L., Thomas D.L., McDonald T.L., Erickson W.P. 2002
544 *Resource selection by animals: statistical design and analysis for field studies*. 2nd ed.
545 Dordrecht, Kluwer Academic Publishers.
546 36. Fithian W., Hastie T. 2013 Finite-sample equivalence in statistical models for
547 presence-only data. *Ann Appl Stat*, 1917-1939. (doi:10.1214/13-AOAS667).
548 37. Aarts G., Fieberg J., Brasseur S., Matthiopoulos J. 2013 Quantifying the effect of
549 habitat availability on species distributions. *J Anim Ecol* **82**, 1135-1145. (doi:10.1111/1365-
550 2656.12061).
551 38. R Core Team. 2013 *R: a language and environment for statistical computing*. R
552 foundation for statistical computing, Vienna, Austria. URL http://www.R-project.org.

553 39. Réale D., Reader S.M., Sol D., McDougall P.T., Dingemanse N.J. 2007 Integrating
554 animal temperament within ecology and evolution. *Biol Rev* **82**, 291-318.
555 (doi:10.1111/j.1469-185X.2007.00010.x).
556 40. Sih A., Bell A.M., Johnson J.C., Ziemba R.E. 2004 Behavioral syndromes: an
557 integrative overview. *Q Rev Biol* **79**, 241-277.
558 41. Verbeek M.E.M., Drent P.J., Wiepkema P.R. 1994 Consistent individual differences
559 in early exploratory behaviour of male great tits. *Anim Behav* **48**, 1113-1121.
560 42. Dall S.R.X., Bell A.M., Bolnick D.I., Ratnieks F.L.W. 2012 An evolutionary ecology
561 of individual differences. *Ecol Lett* **15**, 1189-1198. (doi:10.1111/j.1461-0248.2012.01846.x).
562 43. Bolnick D.I., Yang L.H., Fordyce J.A., Davis J.M., Svanbäck R. 2002 Measuring
563 individual-level resource specialization. *Ecology* **83**, 2936-2941.
564 44. Bolnick D.I., Svanbäck R., J. A. Fordyce, L.H. Yang, J.M. Davis, C. D.Hulsey,
565 M.L. Forister. 2003 The ecology of individuals: incidence and implications of individual
566 specialization. *Am Nat* **161**, 1-28. (doi:10.1086/343878).
567 45. Marchetti K., Price T. 1989 Differences in the foraging of juvenile and adult birds: the
568 importance of developmental constraints. *Biol Rev* **64**, 51-70.
569 46. Bergmüller R., Taborsky M. 2010 Animal personality due to social niche
570 specialisation. *Trends Ecol Evol* **25**, 504-511.
571 47. Bijleveld A.I., Folmer E.O., Piersma T. 2012 Experimental evidence for cryptic
572 interference among socially foraging shorebirds. *Behav Ecol* **23**, 806-814.
573 (doi:10.1093/beheco/ars034).
574 48. van Gils J.A., de Rooij S.R., van Belle J., van der Meer J., Dekinga A., Piersma T.,
575 Drent R. 2005 Digestive bottleneck affects foraging decisions in red knots *Calidris canutus*.
576 I. Prey choice. *J Anim Ecol* **74**, 105-119. (doi:10.1111/j.1365-2656.2004.00903.x).

577 49. Goss-Custard J.D., West A.D., Yates M.G., Caldow R.W.G., Stillman R.A., Bardsley
578 L., Castilla J., Castro M., Dierschke V., le V. dit Durell S.E.A., et al. 2006 Intake rates and
579 the functional response in shorebirds (Charadriiformes) eating macro-invertebrates. *Biol Rev*
580 **81**, 501-529. (doi:10.1017/s1464793106007093).
581 50. Drent R., Swierstra P. 1977 Goose flocks and food finding: field experiments with
582 barnacle geese in winter. *Wildfowl* **28**, 15-20.
583 51. Ydenberg R., Prins H.T. 1981 Spring grazing and the manipulation of food quality by
584 barnacle geese. *J Appl Ecol* **18**, 443-453.
585 52. Drent R.H., van der Wal R. 1999 Cyclic grazing in vertebrates and the manipulation
586 of the food resources. In *Plants, Herbivores, and Predators* (eds. Olff H., Brown V.K., Drent
587 R.H.), pp. 271-299. Oxford, Blackwell Science Ltd.
588 53. Bijleveld A.I., MacCurdy R., Chan Y.-C., Penning E., Gabrielson R., Cluderay J.,
589 Spaulding E., Dekinga A., Holthuijsen S., Ten Horn J., et al. (2016) Data from:
590 Understanding spatial distributions: Negative density-dependence in prey causes predators to
591 trade-off prey quantity with quality. Dryad Data Repository.
592 http://dx.doi.org/10.5061/dryad.d75hq
593

Figure captions

Fig. 1 A trophic pyramid for our study system. Within trophic layers negative density-dependence has been studied in the context of population regulation. For instance, as population size increases an individual's state (e.g., body mass) decreases, which negatively affects their reproductive output and survival probability. Here, we focus on the effects that negative density-dependence among prey has on their predators. Negative density-dependence occurs within all trophic levels. Likewise, the effects of density dependence occur between all trophic levels. Dashed lines represent negative interaction pathways, and solid lines represent positive interaction pathways. The red arrow represents the focus of this study, i.e. the between trophic-level effect of density dependence on body mass. Photo courtesy: Jan van de Kam (*Falco peregrinus* and *Calidris canutus*), Allert Bijleveld (*Cerastoderma edule)*, and NIOZ (collection of phytoplankton species).

Fig. 2 Negative density-dependence in cockle flesh mass caused a hump-shaped functional response for knots (a type IV functional response). (A) A cockle's relative ash-free dry mass of the flesh ($AFDM_{flesh}$) plotted against cockle density (m^{-2}). The regression line reflects the statistical model presented in Online Supplementary Table S1A. (B) The predicted energy functional responses of knots foraging on 7 mm long cockles (thick black line), which includes the negative density-dependence in relative cockle $AFDM_{flesh}$ (short-dashed line with units on the right y-axis). We also plotted the Holling type II functional response without the negative density-dependence among cockles (long-dashed line). For reference, we included the threshold intake rate that knots need to acquire energy balance [grey horizontal line, 34].

Fig. 3 Resource landscapes with the low-tide distribution of knots. The panels show interpolated (A) cockle densities (m^{-2}), (B) relative flesh masses of cockles ($AFDM_{flesh}$), (C) predicted intake rates of knots (IR, mg $AFDM_{flesh}$ s^{-1}), and (D) average gizzard-mass-dependent predicted intake rates ($IR_{avg.gizzard}$, mg $AFDM_{flesh}$ s^{-1}). The panels additionally show the residence patches of all tagged knots. The sizes of these symbols indicate how long a bird had spent in that particular location ranging from 10 min to 4.7 h. The underlying satellite imagery was obtained from Bing in the QGIS OpenLayers plugin.

Fig. 4 Knot resource selection functions. All panels show the resource selection functions on the y-axis, which are proportional to the probability of knot occurrence. The different panels have different prey related predictor variables on the x-axis: (A) cockle density (m^{-2}), (B) relative cockle flesh mass ($AFDM_{flesh}$), (C) predicted knot intake rates without a digestive constraint (IR, mg $AFDM_{flesh}$ s^{-1}), (D) average gizzard-mass-dependent predicted intake rates ($IR_{avg.gizzard}$, mg $AFDM_{flesh}$ s^{-1}), and (E) individual gizzard-mass-dependent predicted intake rates ($IR_{ind.gizzard}$, standardised). Note that these resource selection functions are the exponent of fitted logistic regression models excluding the intercepts (Online Supplementary Table S3). As a result, for instance, the linear model in Online Supplementary Table S3E becomes curved in (panel E).

Figures

Fig. 1

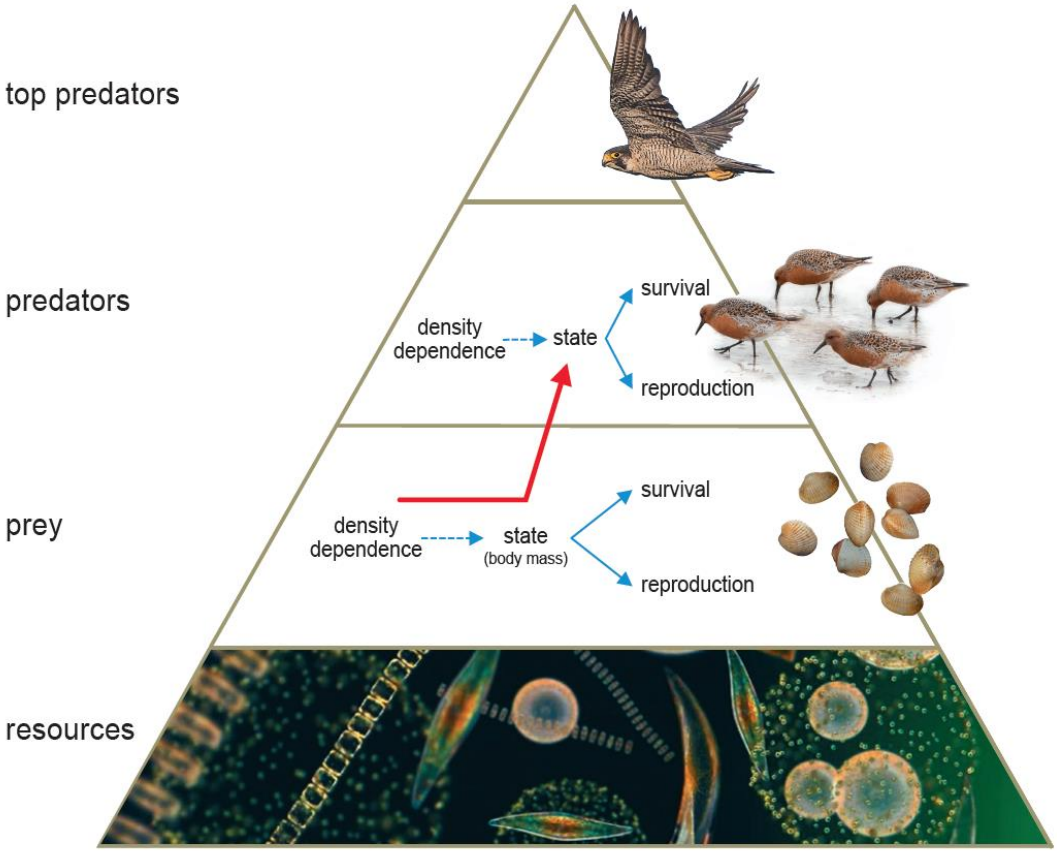

641 **Fig. 2**

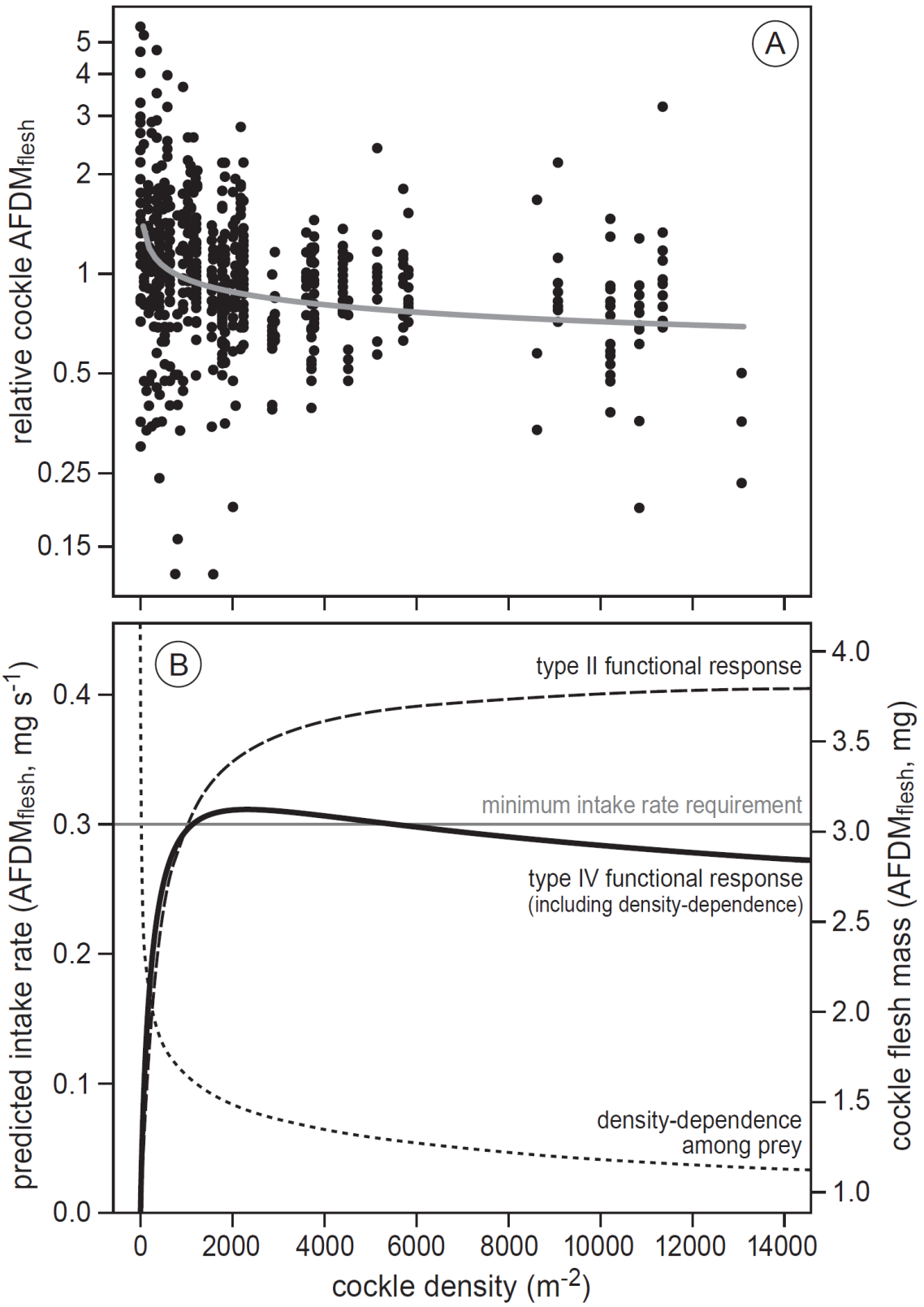

642
643

644 **Fig. 3**

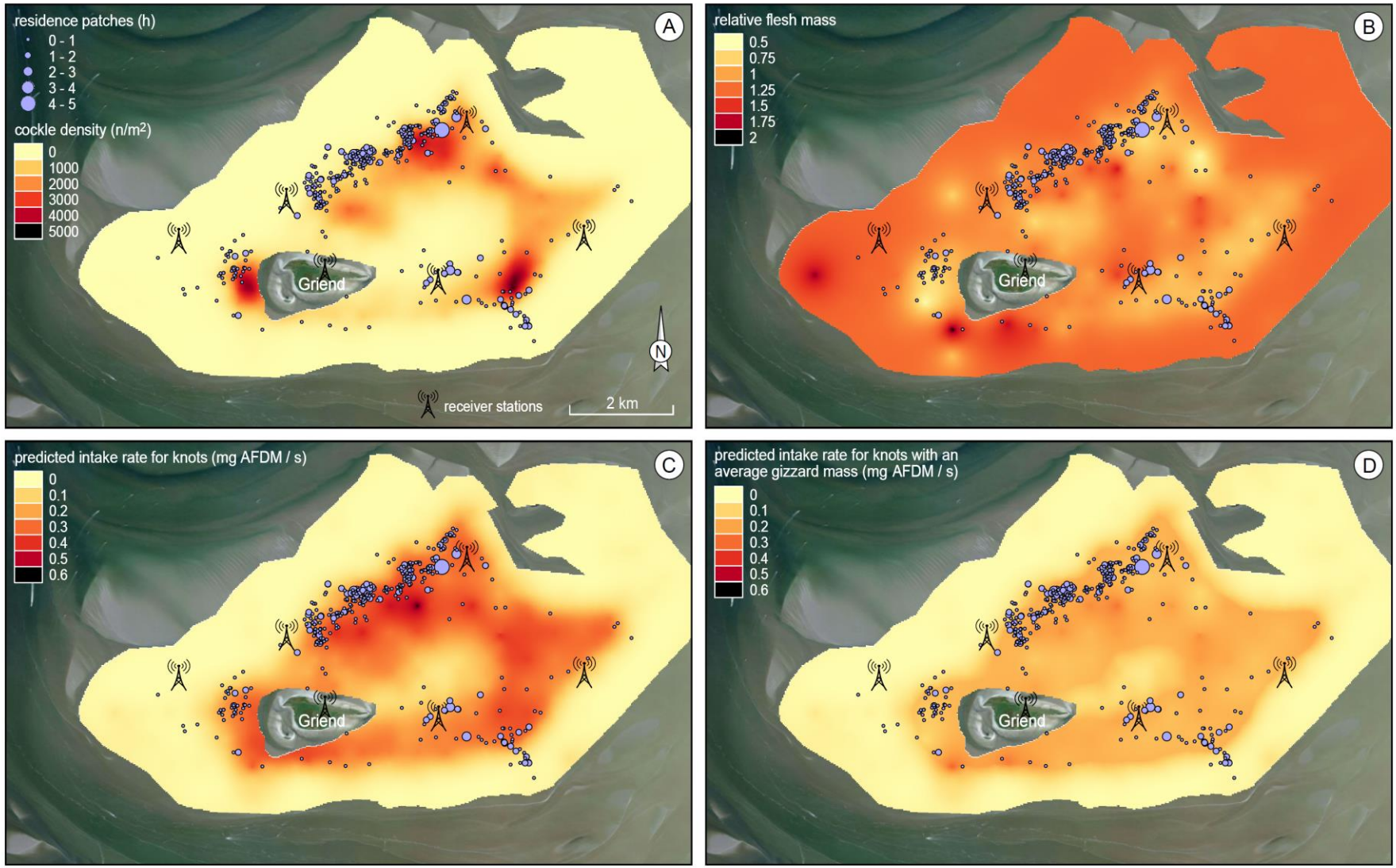
residence patches (h)
0 - 1
1 - 2
2 - 3
3 - 4
4 - 5
cockle density (n/m²)
0
1000
2000
3000
4000
5000
A
Griend
N
receiver stations
2 km
relative flesh mass
0.5
0.75
1
1.25
1.5
1.75
2
B
Griend
predicted intake rate for knots (mg AFDM / s)
0
0.1
0.2
0.3
0.4
0.5
0.6
C
Griend
predicted intake rate for knots with an average gizzard mass (mg AFDM / s)
0
0.1
0.2
0.3
0.4
0.5
0.6
D
Griend

645

646 **Fig. 4**

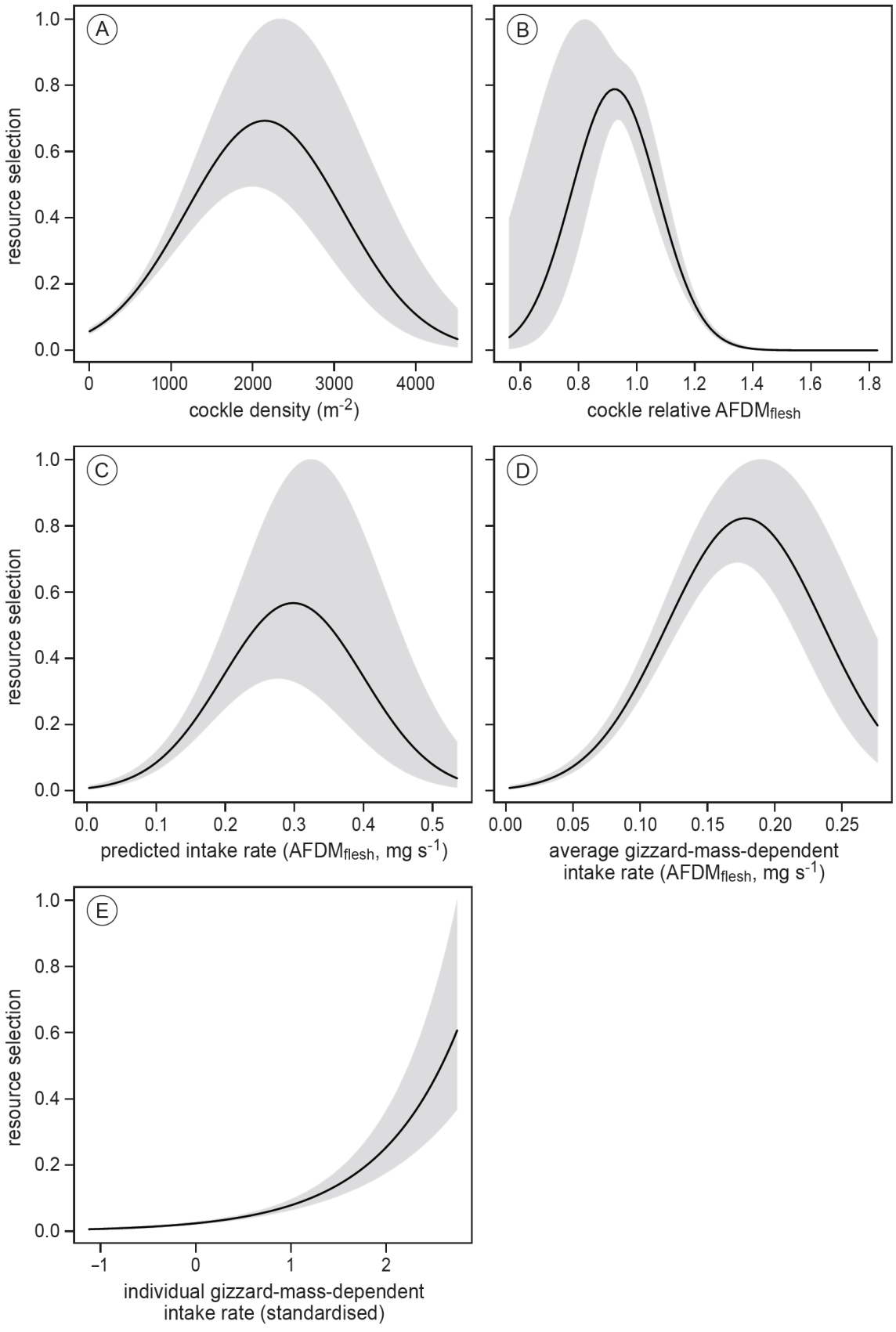
A
B
C
D
E
resource selection
1.0
0.8
0.6
0.4
0.2
0.0
0
1000
2000
3000
4000
cockle density (m-2)
0.6
0.8
1.0
1.2
1.4
1.6
1.8
cockle relative AFDMflesh
0.0
0.1
0.2
0.3
0.4
0.5
predicted intake rate (AFDMflesh, mg s-1)
0.00
0.05
0.10
0.15
0.20
0.25
average gizzard-mass-dependent intake rate (AFDMflesh, mg s-1)
−1
0
1
2
individual gizzard-mass-dependent intake rate (standardised)

647

Online Supplementary Information for:

Understanding spatial distributions: Negative density-dependence in prey causes predators to trade-off prey quantity with quality

Allert I. Bijleveld, Robert B. MacCurdy, Ying-Chi Chan, Emma Penning, Richard M. Gabrielson, John Cluderay, Eric L. Spaulding, Anne Dekinga, Sander Holthuijsen, Job ten Horn, Maarten Brugge, Jan A. van Gils, David W. Winkler, and Theunis Piersma

Table S1 Mixed-modelling results for density dependence in cockle flesh and shell mass. We analysed the effects of cockle density (m^{-2}) and length (mm) on an individual cockle's (A) relative ash-free dry mass of the flesh ($AFDM_{flesh}$), and (B) relative dry mass of the shell (DM_{shell}). Cockle density was log_{10}-transformed, and covariates were centred on their mean length (8.95 mm) and log_{10}-transformed density (3.14). The random effect estimates refer to standard deviations.

	Response variables	Random	Predictors	Estimates	SE	*P*
(A)	relative $AFDM_{flesh}$		intercept	-0.03	0.02	0.16
			density	-0.14	0.02	<0.01
			length	-0.00	0.00	0.52
			density × length	0.00	0.00	0.25
		sampling station		0.15		
		Residual		0.16		
(B)	relative DM_{shell}		intercept	-0.01	0.02	0.75
			density	-0.06	0.03	0.04
			length	-0.00	0.00	0.97
			density × length	0.00	0.00	0.38
		sampling station		0.04		
		residual		0.04		

Table S2 Model selection results for the shape of resource selection functions. We analysed the same response variable with different types of prey related explanatory variables (resource landscapes): (A) cockle density (m^{-2}), (B) relative cockle ash-free dry mass of the flesh ($AFDM_{flesh}$), (C) predicted intake rates (IR, mg $AFDM_{flesh}$ s^{-1}), (D) average gizzard-mass-dependent predicted intake rates ($IR_{avg.gizzard}$, mg $AFDM_{flesh}$ s^{-1}), and (E) individual gizzard-mass-dependent predicted intake rate ($IR_{ind.gizzard}$, standardised). In order to analyse the shape of knot 'Resource Selection Functions' (RSF), we compared linear and quadratic models to the null model (intercept only). We avoided collinearity between the linear and quadratic terms by calculating orthogonal polynomials. To compare the different shapes of RSF, we calculated the log-likelihood of models by cross validation as follows [1]: We treated the 13 individuals as independent sampling units, and by excluding one individual at a time, fitted the resource selection model to this 'training' data. With this fitted model, we predicted the response of the excluded individual and calculated the log-likelihood in comparison to its observed response data. We repeated this procedure for all individuals and summed their log-likelihoods. The null-model with only an intercept had a log-likelihood of -1365.3. Comparing the log-likelihoods revealed that (as indicated in bold) the quadratic resource selection function was the best model for cockle density, relative $AFDM_{flesh}$, IR, as well as $IR_{avg.gizzard}$. Conversely, the linear model described the $IR_{ind.gizzard}$ resource selection function best. Note that the linear and quadratic terms were also imposed on the random effects (random slopes mixed-effect modelling).

	Resource landscapes	RSF shape	Log-Likelihood
(A)	cockle density (m^{-2})	linear	-1272.0
		quadratic	-1208.7
(B)	relative cockle $AFDM_{flesh}$	linear	-1257.2
		quadratic	-1208.0
(C)	predicted intake rate (IR, mg $AFDM_{flesh}$ s^{-1})	linear	-1178.0
		quadratic	-1123.3
(D)	average gizzard-mass-dependent intake rate ($IR_{avg.gizzard}$, mg $AFDM_{flesh}$	linear	-1175.6
		quadratic	1137.9
(E)	individual gizzard-mass-dependent intake rate ($IR_{ind.gizzard}$, standardised)	**linear**	-1171.1
		quadratic	-1184.5

Table S3 Parameter estimates of the best supported resource selection functions. (A) cockle density (m^{-2}), (B) relative cockle ash-free dry mass of the flesh ($AFDM_{flesh}$), (C) predicted intake rates (IR, mg $AFDM_{flesh}$ s^{-1}), (D) average gizzard-mass-dependent predicted intake rates ($IR_{avg.gizzard}$, mg $AFDM_{flesh}$ s^{-1}), and (E) individual gizzard-mass-dependent predicted intake rates ($IR_{ind.gizzard}$, standardised). We provide the fixed-effect estimates that represent the average response, and random-effect estimates that represent the individual variation in responses. Note that the estimates of the random effects are given in standard deviations.

	Resource landscape	Model part	Predictors	Estimates	SE
(A)	cockle density (m^{-2})	fixed	intercept	-9.4	0.05
			linear	53.3	6.04
			quadratic	-33.1	3.45
		random	intercept	0.0	
			linear	19.1	
			quadratic	7.6	
(B)	relative cockle $AFDM_{flesh}$	fixed	intercept	-9.8	0.07
			linear	-98.9	5.21
			quadratic	-59.8	11.87
		random	intercept	0.0	
			linear	5.3	
			quadratic	38.0	
(C)	predicted intake rates (IR, mg $AFDM_{flesh}$ s^{-1})	fixed	intercept	-10.2	0.17
			linear	122.8	14.56
			quadratic	-43.9	3.63
		random	intercept	0.5	
			linear	46.7	
			quadratic	2.9	
(D)	average gizzard-mass-dependent predicted intake rates ($IR_{avg.gizzard}$, mg $AFDM_{flesh}$ s^{-1})	fixed	intercept	-10.2	0.12
			linear	136.1	9.43
			quadratic	-36.4	4.26
		random	intercept	0.0	
			linear	16.7	
			quadratic	6.9	
(E)	individual gizzard-mass-dependent predicted intake rates ($IR_{ind.gizzard}$, standardised)	fixed	intercept	-9.7	0.09
			linear	91.1	7.92
		random	intercept	0.2	
			linear	23.1	

Appendix S1

Details on cockle sampling and how we measured cockle flesh and shell mass. At each sampling site we collected 0.018 m^2 of mudflat to a depth of 30 cm. Judging their length in the field, we stored cockles < 8 mm in a 4% formaldehyde solution, and froze larger cockles [2]. The cockles were often too small to separate their flesh from their shell. In those cases, we measured ash-free dry mass of whole individuals ($AFDM_{total}$). To acquire $AFDM_{flesh}$ for these individuals, we subtracted ash-free dry mass of the shell ($AFDM_{shell}$) from $AFDM_{total}$. We estimated $AFDM_{shell}$ in mg from length as $0.0047 \times mm^{2.78}$ [3]. To reduce measurement error in $AFDM_{flesh}$ of small cockles, we pooled similarly sized cockles and calculated average $AFDM_{flesh}$.

Fig. S1

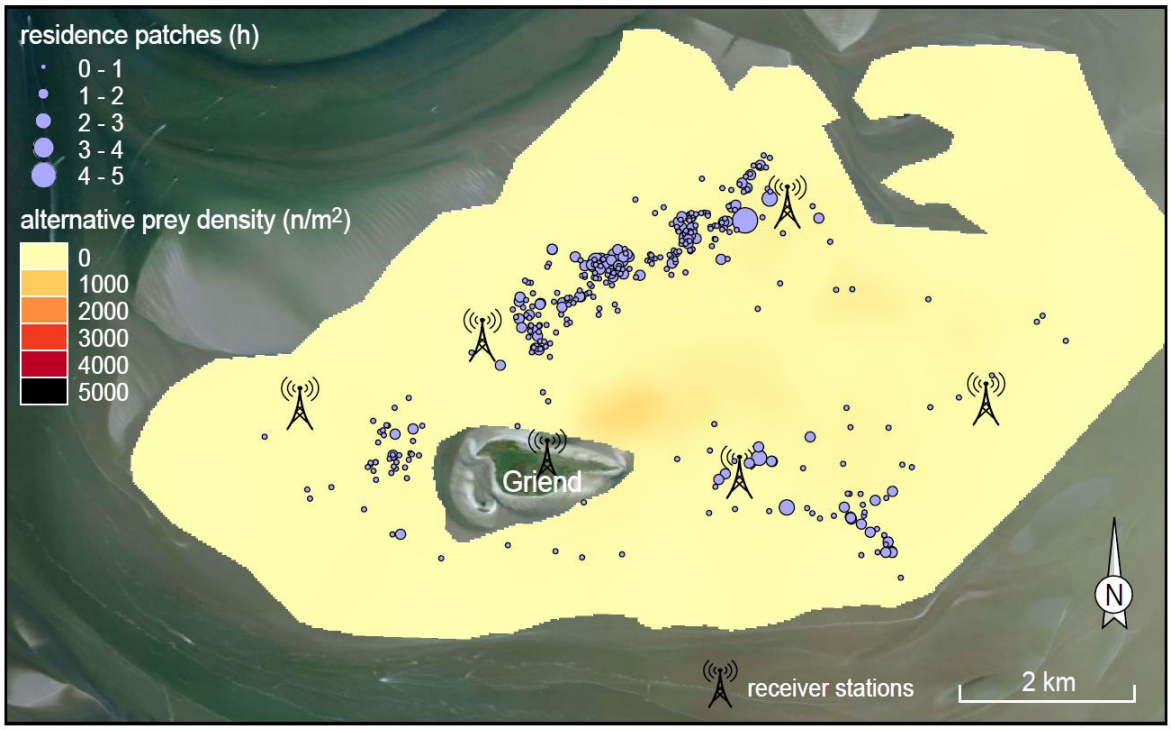

The spatial distribution of alternative prey densities. The average density of alternative prey was 33 m^{-2} (95%CI [9.6; 63.7]) and low compared to those of edible cockles (Fig. 3A). Of the prey occurring in our sampling cores, knots are known to forage on Balthic tellins (*Macoma balthica*), sand gapers (*Mya arenaria*), and *Abra tenuis*. We selected individuals of these species, which knots could swallow (length < 18 mm, [4]), summed the numbers of individuals per sampling core, and calculated densities as described in the Methods for edible cockles (*Cerastoderma edule*).

Fig. S2

Sampling methodology. (A) Photo of a tagged knot moments after its release, and (B) an overview of the study area with the array of (9) receiver stations and sampling stations. We calculated cockle densities for all sampling stations, and when cockles were found we also measured their lengths. From a subset of sampling stations, we additionally measured cockle flesh and shell mass. These stations are indicated in orange. The underlying satellite imagery was obtained from Bing in the QGIS OpenLayers plugin.

Fig. S3

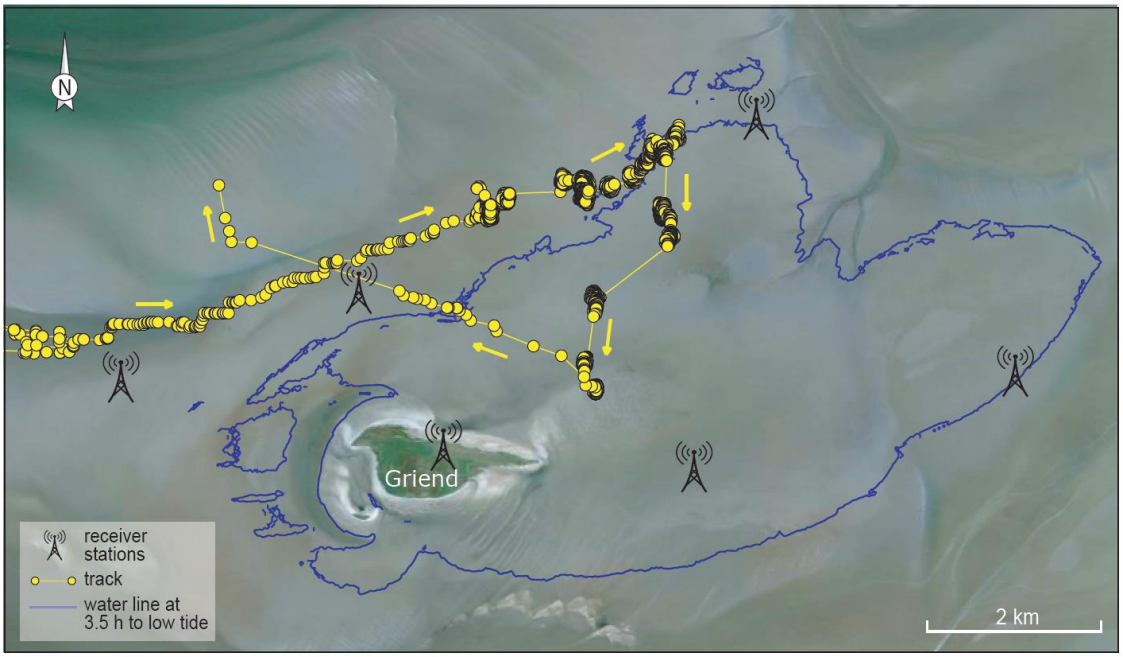

A characteristic knot movement pattern around low tide. This track was measured on 15 August 2011. The dots represent estimated positions that are connected by lines, and the arrows indicate the direction of movement. After roosting nearby on Richel (see Online Supplementary Fig. S2B) and by the time the receding water level had exposed suitable foraging grounds, the bird arrived on the mudflats north of Griend and carried on towards the northeast. With the incoming tide, it moved to the elevated mudflats northeast of Griend before flying back to Richel. The underlying satellite imagery was obtained from Bing in the QGIS OpenLayers plugin.

Fig. S4

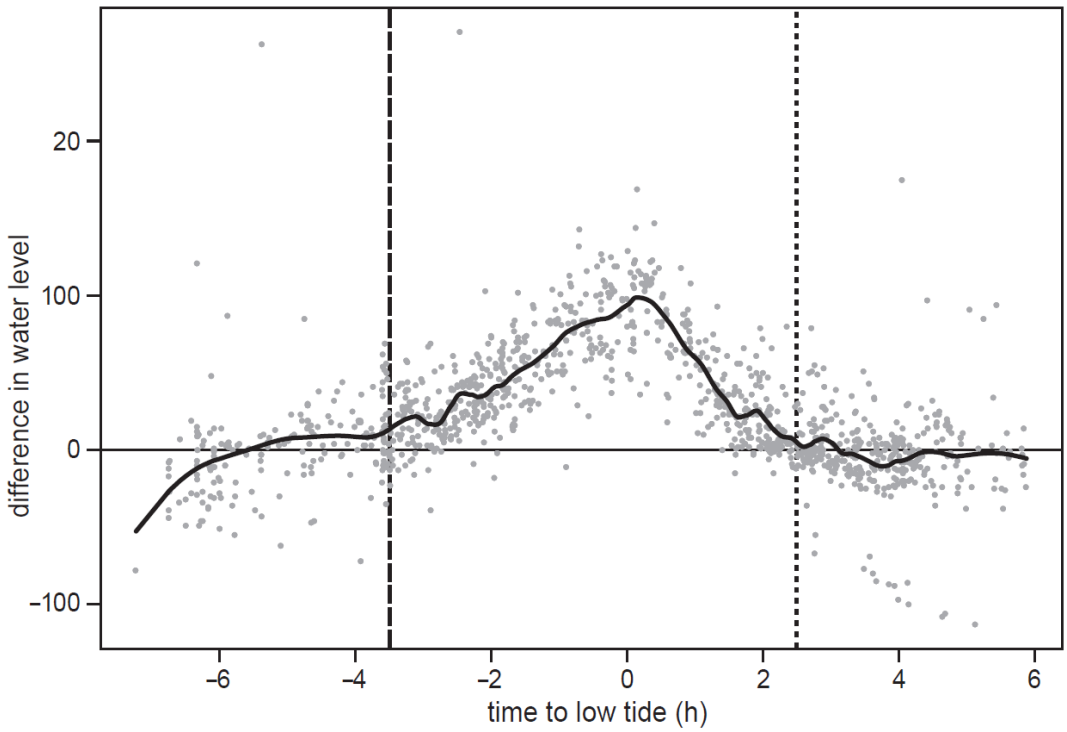

Tidal forcing on the spatial distributions of knots. Each dot represents a residence patch. The y-axis shows the difference (cm) between the water level and the height of the mudflat where the birds were located (residence patches). A positive difference indicates that birds were located on exposed mudflat. Negative values indicate that birds were standing in the water. The time to low tide (h) is shown on the x-axis. The solid line is a LOESS-fit to guide the eye. Between the long-dashed and short-dashed line there was minimal tidal forcing and the birds were more or less free to choose where to forage. The tidal data were collected by Rijkswaterstaat at West-Terschelling (53°21.45'N, 5°13.13'E) at an interval of 10 min (http://www.rijkswaterstaat.nl). The heights of the mudflats were obtained from Rijkswaterstaat as well and were collected between 2003-2008.

Fig. S5

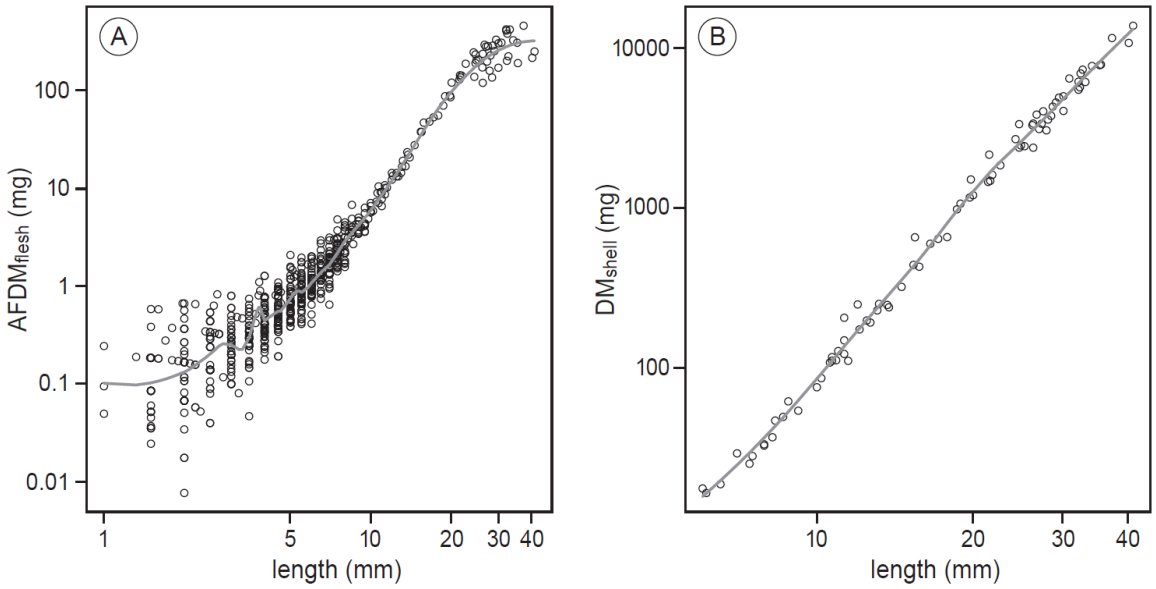

Allometric relations for cockle (A) ash-free dry mass of the flesh ($AFDM_{flesh}$), and (B) dry mass of the shell (DM_{shell}). Because of remaining non-linearity in these allometric relationships, we fitted non-linear local regression models (LOESS, solid lines) on log-log scales [5]. We used smoothing parameters of 0.2 and 0.5 for the LOESS models visualized in respectively panels A and B. We obtained an individual's relative $AFDM_{flesh}$ and DM_{shell} by back-transforming its residual from these LOESS regression models.

Fig. S6

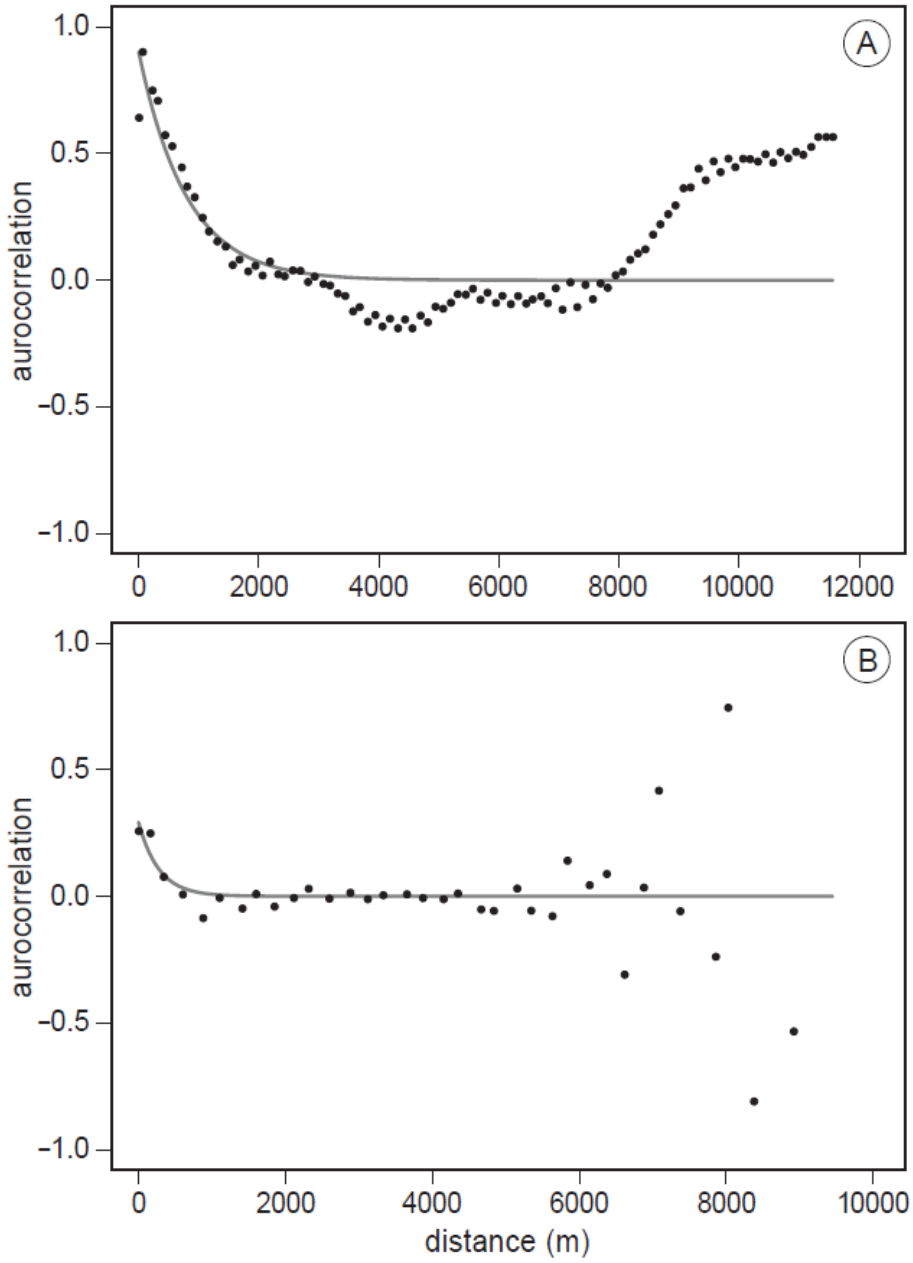

Spatial autocorrelation functions (correlograms) underlying the resource landscapes. In (A) we present the correlogram for cockle density. In (B) we present the correlogram of a cockle's relative ash-free dry mass of flesh ($AFDM_{flesh}$). The spatial autocorrelation function for density is given by $y = 0.90e^{-0.001x}$, and for relative $AFDM_{flesh}$ by $y = 0.29e^{-0.004x}$. For calculating the correlograms, we chose a spatial lag of half that of the inter-sampling distance, i.e. 125 m for interpolating densities and 250 m for interpolating relative $AFDM_{flesh}$.

Fig. S7

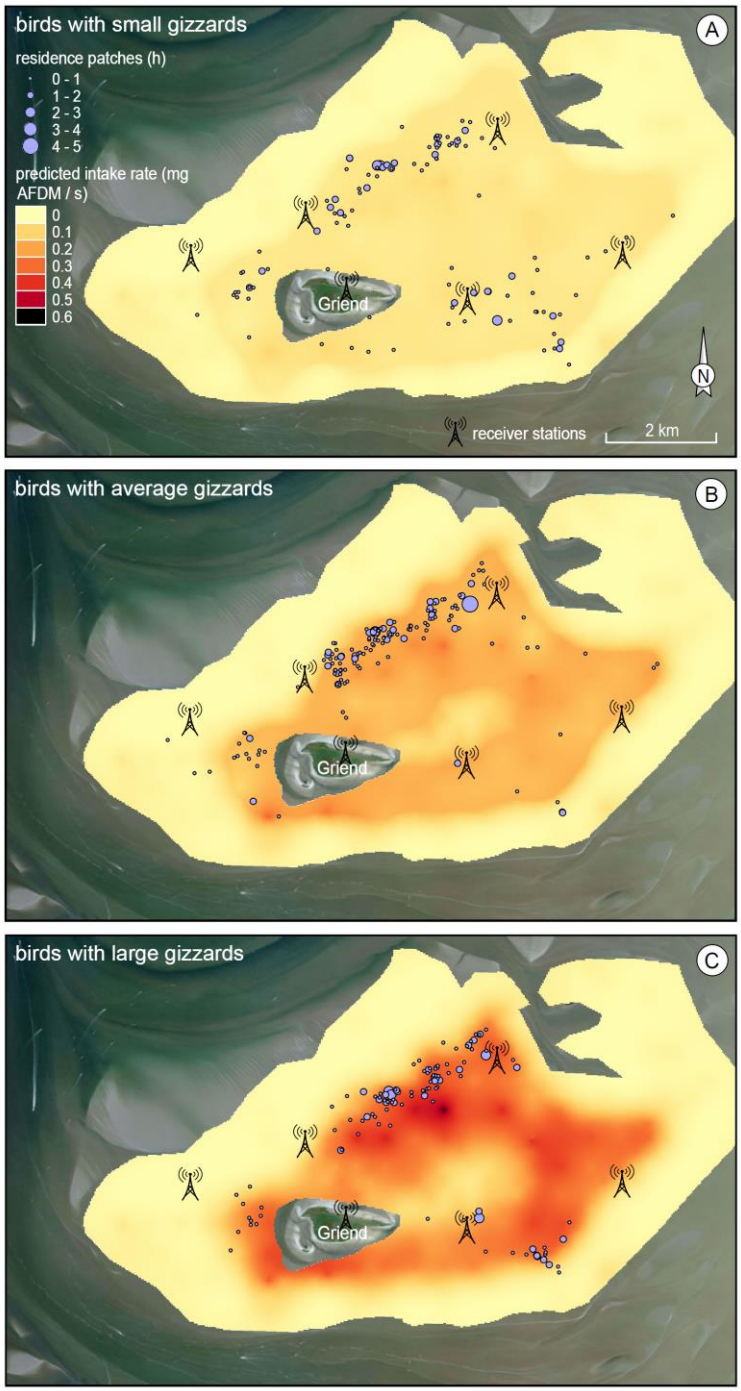

Individual gizzard-mass-dependent predicted intake rates ($IR_{ind.gizzard}$). We plotted the $IR_{ind.gizzard}$ landscapes for three hypothetical birds: (A) a bird with a small gizzard (4 gram), (B) an average gizzard (7 gram), and (C) a large gizzard (10 gram). In order to visualise the difference in predicted intake rates between birds with differently sized gizzards, we used the same colour scaling between panels. We additionally plotted the residence patches of the tagged knots with (A) gizzards < 6 g, (B) gizzards > 6 g and < 8 g, and (C) gizzards > 8 g.

773 The sizes of these residence patch symbols indicate how long a bird had spent in that
774 particular location ranging from 10 min to 4.7 h. Note that the resource landscape of panel B
775 is identical to Fig. 3D. The underlying satellite imagery was obtained from Bing in the QGIS
776 OpenLayers plugin.

Fig. S8

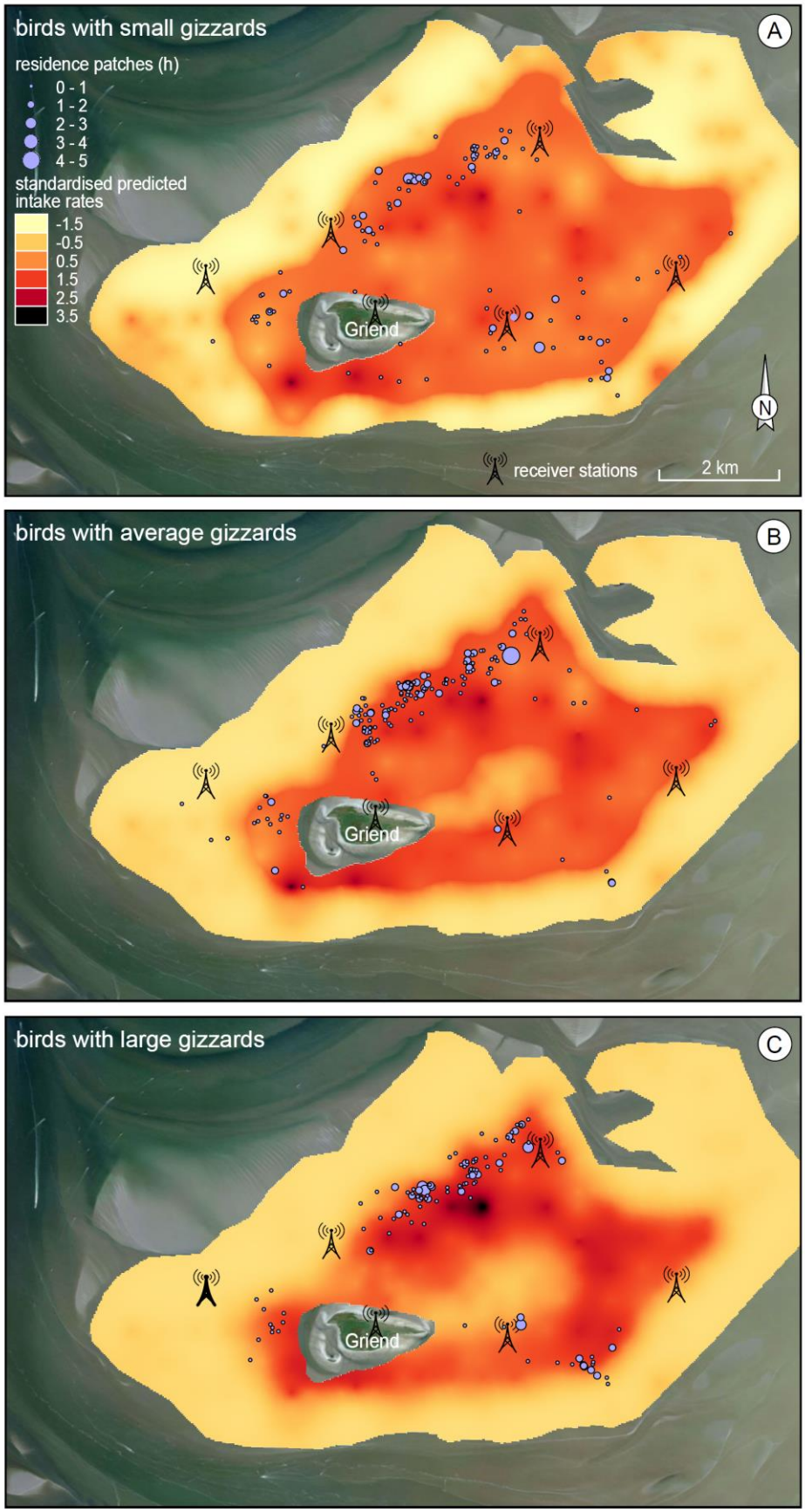
birds with small gizzards
A
residence patches (h)
0 - 1
1 - 2
2 - 3
3 - 4
4 - 5
standardised predicted intake rates
-1.5
-0.5
0.5
1.5
2.5
3.5
Griend
N
receiver stations
2 km
birds with average gizzards
B
Griend
birds with large gizzards
C
Griend

778

Resource landscapes of an individual‘s gizzard-mass-dependent predicted intake rates ($IR_{ind.gizzard}$, standardised). We plotted the standardised $IR_{ind.gizzard}$ landscape for three hypothetical birds: (A) a bird with a small gizzard (4 gram), (B) an average gizzard (7 gram), and (C) a large gizzard (10 gram). We superimposed the residence patches of the tagged birds with (A) gizzards < 6 g, (B) gizzards > 6 g and < 8 g, and (C) gizzards > 8 g. The sizes of these residence-patch symbols indicate how long a bird had spent in that particular location ranging from 10 min to 4.7 h. Note that the resource landscape in panel B is the standardised resource landscape of Fig. 3D. The underlying satellite imagery was obtained from Bing in the QGIS OpenLayers plugin.

Fig. S9

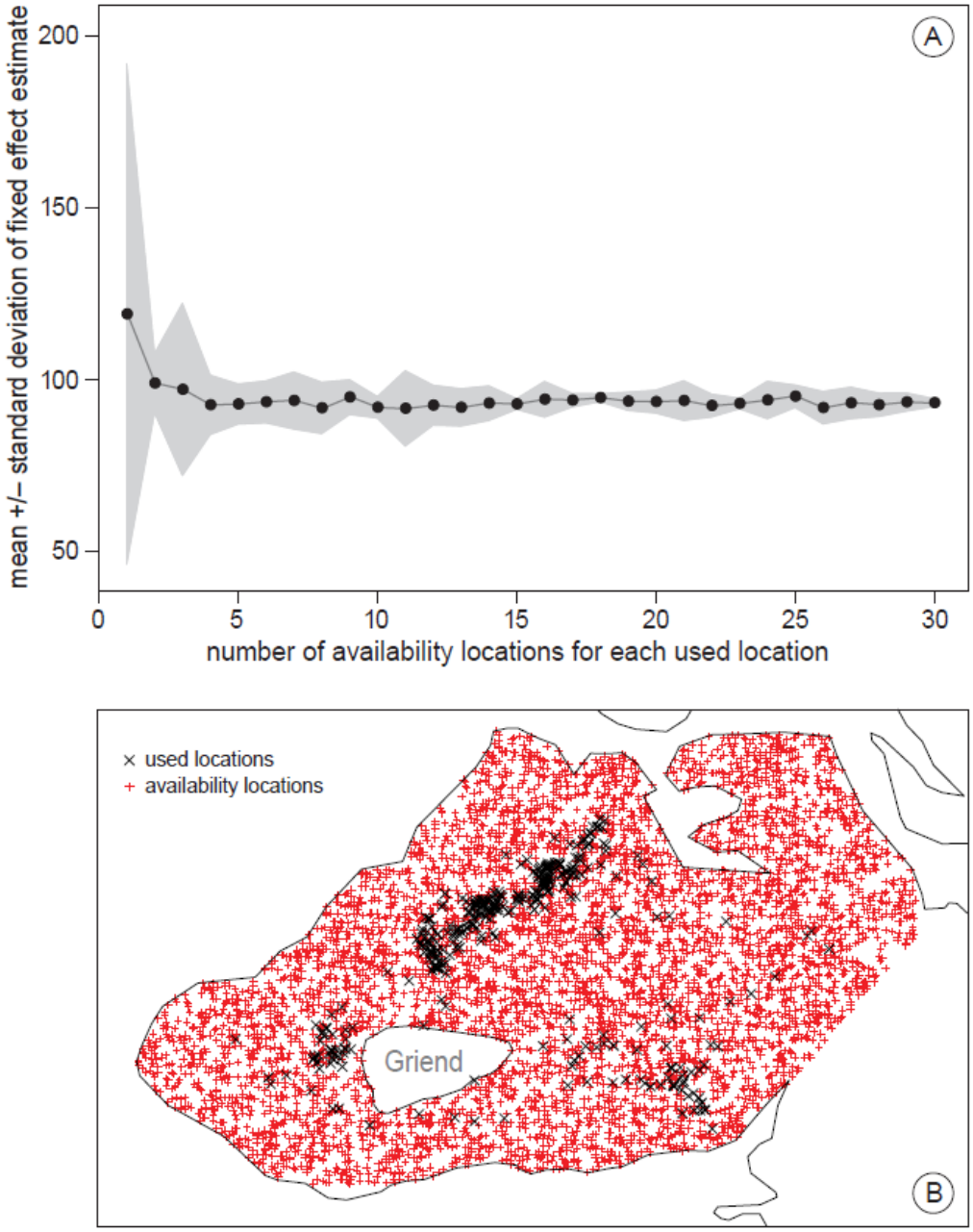

Methodology of the used-availability analyses. In order to determine the number of randomly selected availability locations, we conducted a sensitivity analysis on the fixed-effect parameter estimates. (A) An example of the sensitivity analyses on resource selection modelling. Here, we show the standard deviation (based on 5 estimates) of the linear fixed-effect estimate of the individual-gizzard-mass dependent predicted intake rate model ($IR_{ind.gizzard}$). The x-axis gives the number of availability locations for each used location. The mean of the fixed-effect and its standard deviation levelled off with the ratio of availability

799 locations to used locations; we selected a ratio of 15 that provides reliable model estimates.
800 (B) Map of the used and availability locations underlying our resource selection analyses.

Fig. S10

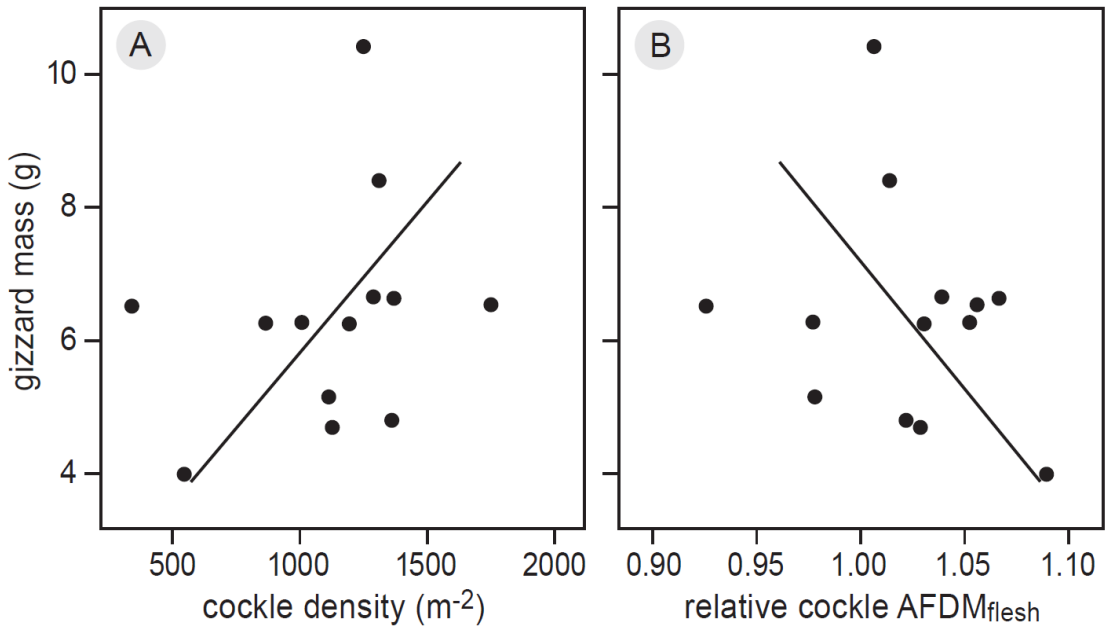

Resource selection in relation to gizzard mass. In Fig. 4E we statistically showed that knots selected those locations where they maximised their gizzard-mass-dependent energy intake rate. To intuitively illustrate that knots with different gizzard masses indeed selected locations with different cockle density and relative ash-free dry mass of the flesh ($AFDM_{flesh}$), we plot an individual's gizzard mass against its average selected (A) cockle density, and (B) relative $AFDM_{flesh}$. Indicative of a trade-off between the quantity and quality of cockle prey, we found a positive correlation between gizzard mass and cockle density, but a negative correlation between gizzard mass and relative $AFDM_{flesh}$. Each dot represents an individual. We calculated average selected cockle density and relative $AFDM_{flesh}$by first averaging within tides and then between tides. The lines represent best-fits from standardized major axis analyses [6] calculated with the R-package "smatr".

Fig. S11

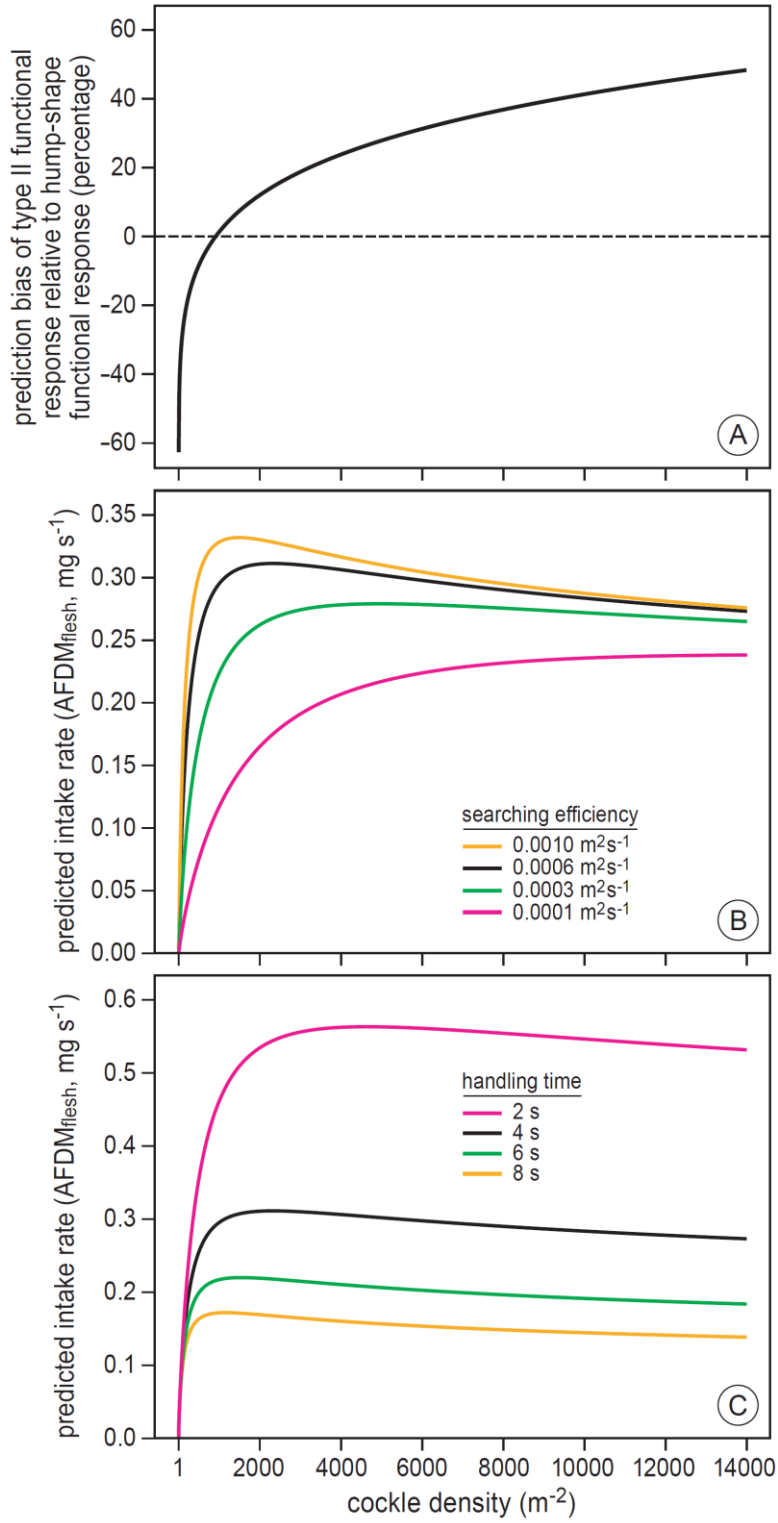

Sensitivity analyses of the type IV functional response. (A) Bias in predicted intake rates when ignoring negative density-dependence in flesh mass among prey. We calculated the difference between predicted intake rates with and without negative density dependence, and

820 show this difference as a percentage of predicted intake rates including negative density-
821 dependence. This bias did not differ between model parameters (searching efficiencies and
822 handling times) of the functional response. (B) The effect of searching efficiency on the
823 functional response while fixing handling time at 4 s. (C) The effect of handling time on the
824 functional response while fixing searching efficiency at 0.00064 $m^2 s^{-1}$. Note that we assumed
825 equal strengths of density dependence in these sensitivity analyses, and that black lines
826 indicate parameter values equal to those used and found in our current study.
827

828 # References

829 1. Aarts G., Fieberg J., Brasseur S., Matthiopoulos J. 2013 Quantifying the effect of
830 habitat availability on species distributions. *J Anim Ecol* **82**, 1135-1145. (doi:10.1111/1365-
831 2656.12061).
832 2. Compton T.J., Holthuijsen S., Koolhaas A., Dekinga A., ten Horn J., Smith J.,
833 Galama Y., Brugge M., van der Wal D., van der Meer J., et al. 2013 Distinctly variable
834 mudscapes: distribution gradients of intertidal macrofauna across the Dutch Wadden Sea. *J*
835 *Sea Res* **82**, 103-116. (doi:10.1016/j.seares.2013.02.002).
836 3. Zwarts L. 1991 Seasonal-variation in body-weight of the bivalves *Macoma balthica,*
837 *Scrobicularia plana, Mya arenaria* and *Cerastoderma edule* in the Dutch Wadden Sea. *Neth*
838 *J Sea Res* **28**, 231-245.
839 4. Piersma T., Hoekstra R., Dekinga A., Koolhaas A., Wolf P., Battley P.F., Wiersma P.
840 1993 Scale and intensity of intertidal habitat use by knots *Calidris canutus* in the Western
841 Wadden Sea in relation to food, friends and foes. *Neth J Sea Res* **31**, 331-357.
842 5. Bijleveld A.I., Twietmeyer S., Piechocki J., van Gils J.A., Piersma T. 2015 Natural
843 selection by pulsed predation: survival of the thickest. *Ecology* **96**, 1943-1956.
844 (doi:10.1890/14-1845.1).
845 6. Smith R.J. 2009 Use and misuse of the reduced major axis for line-fitting. *Am J Phys*
846 *Anthropol* **140**, 476-486. (doi:10.1002/ajpa.21090).

847
848